AN INVESTIGATION ON RESIDUAL STRESS BUILD-UP IN COLD SPRAYED METALLIC SAMPLES: EFFECT OF STRESS RELAXATION HEAT TREATMENT

A Thesis
Submitted to the Graduate Faculty
of the
North Dakota State University
of Agriculture and Applied Science

By

Deepika Shrestha

In Partial Fulfillment of the Requirements
for the Degree of
MASTER OF SCIENCE

Major Department:
Mechanical Engineering

July 2022

Fargo, North Dakota

North Dakota State University
Graduate School

Title

AN INVESTIGATION ON RESIDUAL STRESS BUILD-UP IN COLD SPRAYED METALLIC SAMPLES: EFFECT OF STRESS RELAXATION HEAT TREATMENT

By

Deepika Shrestha

The Supervisory Committee certifies that this ***disquisition*** complies with North Dakota State University's regulations and meets the accepted standards for the degree of

MASTER OF SCIENCE

SUPERVISORY COMMITTEE:

Dr. Fardad Azarmi
Chair

Dr. Annie Tangpong
Co-Chair

Dr. Ali Amiri

Dr. Zhibin Lin

Dr. Sulaymon Eshkabilov

Approved:

August 14, 2022
Date

Dr. Alan Kallmeyer
Department Chair

ABSTRACT

Residual stress formation during cold spraying process may result in deteriorative effects on the performance of coating materials. The objective of this investigation is to characterize residual stress built-up in some of well-known metallic alloys deposited by cold spraying. Two different nickel based super alloys (Inconel 625 and Inconel 718) and the most commercially used titanium alloy (Ti-6Al-4V) were considered for investigation in this study. The average residual stress was higher in Inconel samples compared to titanium one. However, the recovery of residual stress was highest in Ti-6Al-4V compared to nickel-based samples. Mechanical properties such as hardness, porosities and crack formation were investigated in all samples and tribological behavior of Ti-6AL-4V was particularly studied. The relation between the crack formation and residual stress before and after heat treatment was established for Inconel samples. It was tried to define same relationship for wear resistance and residual stress in Ti-6Al-4V sample.

ACKNOWLEDGMENTS

First, I would like to thank "ND NASA EPSCoR" for sponsoring this project. Next, I would like to thank Dr. Fardad Azarmi, my adviser and committee chairman and, my co-adviser Dr. Annie Tangpong. Dr. Azarmi's guidance and mentorship allowed me to succeed and was proven to be invaluable throughout this research. Luke Gibbon is another person well deserving of a thanks as he also provided an immense amount of guidance, and leadership on this project. I would like to thank my committee member Dr. Sulaymon Eshkabilov for his help in my research understanding and motivation. I would also like to express my gratitude to my committee members Dr. Ali Amiri and Dr. Zhibin Lin for helping me shape and achieve this goal.

Finally, I would like to thank all my friends and family who have supported me. I could not have been in this position without your constant support and motivation. I could not be where I am today without the support of everyone on this list and I will be forever grateful.

DEDICATION

To my parents and family.

TABLE OF CONTENTS

LIST OF TABLES

LIST OF FIGURES

LIST OF ABBREVIATIONS

CS.....Cold Spray

APS .....Atmospheric Plasma Spraying

HVOF.....High Velocity Oxygen Fuel

VPS .....Vacuum Plasma Spraying

XRD .....X-ray Diffraction

SLM .....Selective Laser Melting

DLMS .....Direct Metal Laser Sintering

CGDS.....Cold Gas Dynamic Spray Process

SEM .....Scanning Electron Microscopy

LIST OF SYMBOLS

λ.....Wavelength

d.....Crystal spacing in crystallographic planes

θ.....Angular position of diffraction peaks

h.....Planck constant

m .....Mass

L .....Flight path length

Δd.....Change in lattice spacing

d_0 .....Lattice spacing of a stress-free sample

ν.....Speed of the sound

γ.....Ratio of the specific heat

R.....Gas constant

T .....Temperature

1. INTRODUCTION

1.1. Overview

Thermal spraying refers to a family of deposition methods by accelerating molten particles toward a target. Thermal spray processes include various group of technologies that deposit the coatings using concentrated and highly energetic heat source in the form of flame, and plasma jet. Thermal spray processes such as Atmospheric Plasma Spraying (APS), High Velocity Oxygen Fuel (HVOF), Vacuum Plasma Spraying (VPS), wire arc spraying, and cold spraying are among technologies which have been commercialized and widely used by industries. Residual stress, fatigue, and corrosion are among some prominent challenges faced by aeronautical, marine, and automobile industries. In general, in thermal spraying, coatings are produced layer by layer after impact and solidification of the molten particles on the surface of the substrate. The only exception in thermal spraying method is *Cold Spraying* in which coating is built by impact and deformation of solid particles. In fact, Cold spraying is a solid-state deposition technique, where micron sized powders are bonded together with the substrate, attributed to high velocity impact, and associated severe plastic deformation. The solid powder particles are accelerated through a high-pressure nozzle with the convergent-divergent geometry to attain a very high velocity. The cold spray process is performed in temperatures lower than melting point of the metal powders, that ensures the solid-state deposition and provides advantages such as eliminating the risk of melting, oxidation, crystallization and grain growth, and formation of undesirable phases, etc. Due to deposition of coatings in solid condition, the cold spray can be used to deposit thick coatings which is not provided by other thermal spraying technologies. It can also be used for deposition of high-quality metal coatings with structural homogeneity, high density, and high cohesive strength [1,2].

The early technology invented in 1980-1990 was only capable of depositing soft metals such as aluminum and copper while the new high-pressure technology can produce coatings from hard metals such as nickel and titanium alloys. Nickel based superalloys have nickel as their major element with addition of chromium and other elements. They are widely used in many industrial applications, such as aerospace, automobile, power generations. Nickel based superalloys exhibit excellent toughness, corrosion resistance, mechanical properties at elevated temperatures which makes them ideal choice to be used as protective coating material as well. Inconel 718 and Inconel 625 are good examples of nickel-based superalloys that possess high strength properties and protection against corrosion and oxidation [3]. Nickel based coatings such as Inconel 718 and Inconel 625 have been a good solution for strengthening materials used in those applications. HVOF deposited Inconel 625 coatings has shown promising results in terms of improving wear properties in base materials, however, the residual stress formation has been an issue in those coatings [4,5]. Coatings of Inconel 625 has also been deposited using other thermal spray techniques such as air plasma spraying [6], and cold spraying [7]. Inconel 718 coating is a preferred material for repairing of components in aerospace, automobile and nuclear plants which has been mostly deposited using HVOF [8] and cold spraying [3,8-10] technologies.

Titanium and its alloys are also used in many industries such as aerospace, power generations, biomedical, etc. The use of Ti-6Al-4V is more pronounced in biomedical field today because of its higher corrosive resistance, biocompatibility, and high strength to weight ratio. Ti-6Al-4V offers properties such as high strength, high stiffness, fatigue and corrosion resistance, and lower relative density that makes it a good choice for industrial application. These characteristics make Ti-6Al-4V a potential candidate to be used as a coating layer to protect surface of the components in service condition [11]. During service condition, parts are vulnerable to damage

such as wear, dents, corrosion, and cracks. Ti-based components are very expensive and requires a long lead time. For such expensive components, repair and remanufacture of the parts is more desirable and economical. Traditionally, thermal spray techniques have been used for the repair and manufacture purposes. However, thermal spray processes could cause high porosities, oxidation levels at elevated temperatures and high thermal residual stress. To overcome such negative effects, Cold Spray has been a noble and suitable candidate that offers the advantages such as low porosity, low oxidation level and thermal stress and suitability for heat-sensitive materials. These properties make Ti-6Al-4V a suitable candidate not only in terms of mechanical properties but in terms of thermal, and economical point as well. Different thermal spray techniques such as Cold Spraying [12-14], HVOF [15], and Vacuum Plasma Spray [16] deposition has been used for repair of components using Ti-6Al-4V.

Residual stress is considered as a pre-existing stress inside the materials which build up during manufacturing process or it forms due to extreme service condition. The residual stress can form at each step of fabrication process, or it can be built up while in use as an industrial component. The residual stress can be formed in metals and alloys due to mechanical forces exerted to them during production or service. Cold spraying is a good example of possibility for residual stress build up due to the extreme mechanical stresses applied to the particles during high velocity impact. In addition, mechanically generated stress is a known cause in parts when they are subjected to processes such as grinding, milling, machining, welding, etc. Thermally induced residual stresses are build up in the parts and components due to thermal gradients or differences in thermal expansion coefficient. Chemically generated stress can be developed due to volume changes associated with chemical reactions, precipitation, or phase transformation. Chemical surface treatments can lead to the generation of residual stress on the surface layers of component.

Phase change that takes place within the materials causing the misfits in dimension due to volume change, results in the formation of residual stress that commonly occurs during heat treatment process.

1.2. Residual Stress in Thermally Sprayed Coatings

Residual stress in thermal spray coating is important factor that affects the performance of the materials and influence the performance of the coatings. High amount of residual stress prevents deposition of thick coatings and can lead to cracking and delamination of the coatings [17]. The main sources of the residual stresses formation in thermally sprayed coatings can be listed as:

1. Rapid solidification of molten particles (quenching) upon impact on the substrate. As mentioned before, it occurs in thermal spraying technologies which involve increasing temperature above melting point of particles and spraying them at molten condition. The impacted droplets are rapidly solidifying, and this quick phase change can cause stress build-up in deposited coatings [18]. Stresses developed are called ‘intrinsic’, ’deposition’ or ‘quenching’ stresses and these are mainly of tensile nature [19].
2. The temperature gradient and mismatch of the thermal coefficient that leads to the thermal shrinkage during cooling of the deposition layers are the second source of residual stress formation in thermal spray coatings. The so-called thermal mismatch stresses can be tensile or compressive depending upon the sign of the difference and deposition temperature [19].
3. The solid-state impact of the accelerated particles on the substrate and consecutive deposition of the particles may result in severe deformation of the solid powders. The plastic deformation upon the impact induces residual stress build-up in cold sprayed coatings.

Residual stresses can be of tensile or compressive in nature. Sometimes, residual stress is considered desirable for some industries. For example, rapid cooling (quenching) of the glass generates the compressive stress which inhibit the crack formation from the surface. In some cases, only as per its application, compressive stresses are believed to have beneficial effect on adhesion and fatigue strength [20]. However, in many circumstances both compressive and tensile residual stresses are considered undesirable stresses that can lead to cracking and fatigue failure if their magnitude exceeds the tensile strength of the coatings.

Residual stress can also be classified in three different types according to their magnitude [20-21].

1. Residual stress type I

   These are the macro scale stresses varying quasi-continuously across dimensions comparable with the size of component. The characteristics length is commonly measured in millimeters. Pre-stressed concrete or bolted structures are examples of macro-scale stresses.

2. Residual stress type II

   These are the stresses on microstructure on the scale of grain size of the metal. To better understand the material behaviors and improvising of the processing methods, it is important to learn about Type II stresses. The size of Type II stresses is mostly measured in μm scale.

3. Residual stress type III

   These are the stresses on the atomic scale. Stresses within the crystal lattice such as in the region dislocations and different grain boundaries may present in atomic scale. The

characteristic length has the same scale as lattice spacing and they commonly measured in Angstrom.

1.3. Methods of Residual Stress Measurement

Existence of residual stress may be beneficial for some components and could be deliberately induced for parts used in specific applications. For instance, materials subjected to a rapid cooling process such as quenching during glass production may induce a compressive residual stress which can resist the crack formation in the final product [22]. Residual stress, on the other hand, can be detrimental for other materials and produced parts. The tensile residual stress that is induced during the manufacturing of materials, such as welding, machining, grinding, is typically undesirable. To reduce the risk of damage it is important to know about the type and amount of residual stress built up in the materials.

There are several methods for measurement of residual stress within microstructure of materials which can be categorized to two groups of destructive and non-destructive methods. Destructive methods can measure the residual stress at large depth, whereas non-destructive methods are limited to measurement of residual stress to only certain depths. Destructive methods include techniques such as hole drilling, deep hole drilling, contour method, and curvature. For non-destructive methods, commonly used techniques include x-ray diffraction [23], Raman [24], Ultrasonic [25] and neutron diffraction [26].

1.3.1. Destructive Methods

1.3.1.1. Hole Drilling Method

Hole drilling method is one of the most widely used techniques for the determination of residual stress in the superficial layer of the material. It is a standard, relatively simple,

inexpensive, quick, and a well-adapted method for the measurement of residual stress. The basic hole drilling method involves two stages:

1. It starts with drilling of a small hole into the surface of the object at the center of special strain gauge rosette. The schematic of strain gauge rosette is shown in Fig. 1.
2. Measurement of the relieved strain around the hole by means of extensimetric rosette [17].

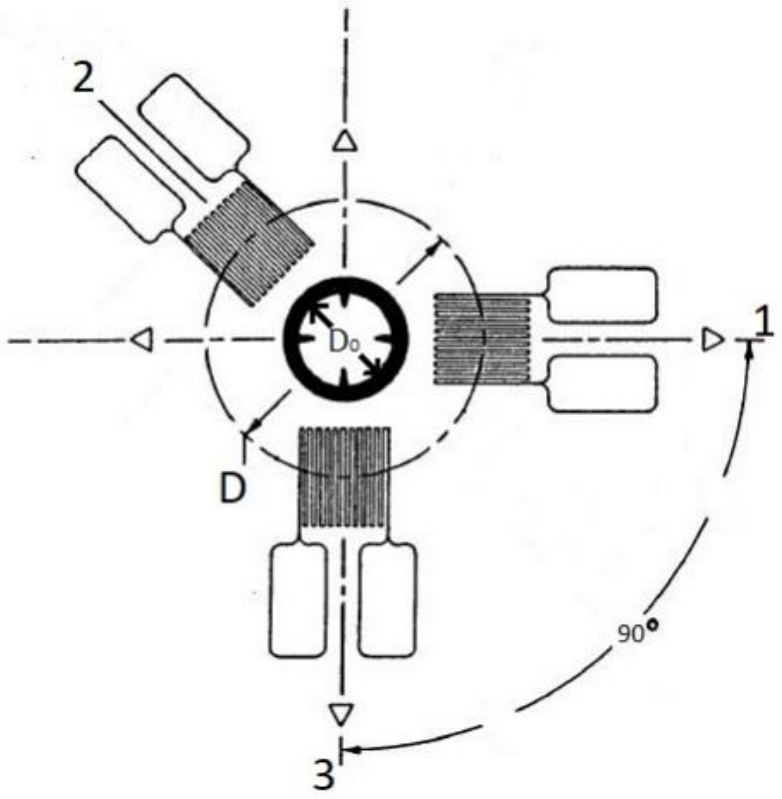

Fig. 1. Schematic diagram of the geometry of a typical 3-element strain gauge rosette [19].

In basic hole drilling method [19], stress may remain constant and uniform throughout the depth of the hole. This technique is an appropriate method for thin specimens. Whereas for the thick samples, incremental hole drilling method is preferred [18].

1.3.1.2. Incremental Hole Drilling

The incremental hole drilling method involves the series of subsequent hole drilling. The incremental hole drilling is carried out by using a high velocity drilling machine shown in Fig. 2,

which provides the reduction in induced stress by drilling and gives accurate measurement of hole size and eccentricity. The machine allows the precise centering of the end mill by means of co-axially assembled microscope for the direct measurement of the hole diameter and eccentricity with a centesimal gauge.

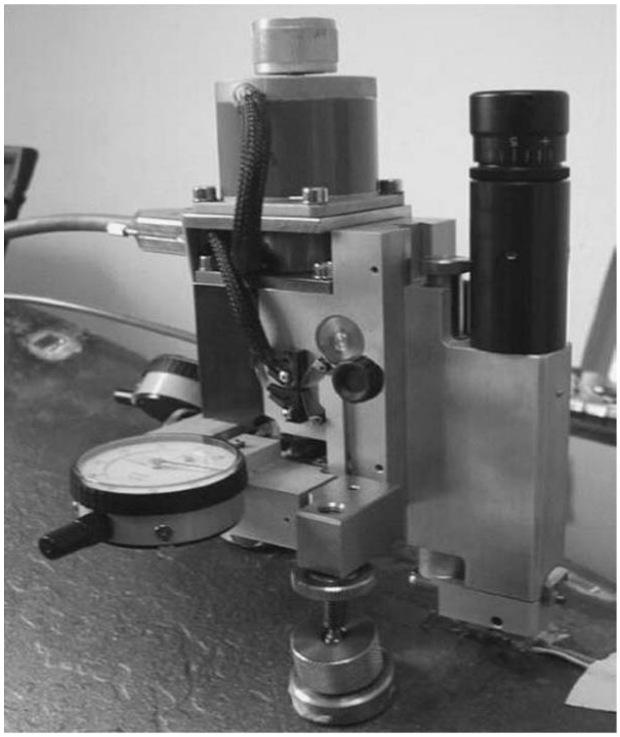

Fig. 2. Incremental hole drilling machine [27].

1.3.1.3. Curvature Method

Curvature method is generally used to measure the average residual stress within the coatings. During the deposition of the coatings on the substrate, residual stress can be induced. The residual stress could cause the substrate to bend as illustrated in Fig. 3. The induced residual stress in the coatings can be calculated through the changes in the curvature. The stress is measured as a function of thickness with the help of strain gauge, profilometer or laser scanning with the accuracy of 0.1 mm^{-1}. The changes in the resulting curvature during the deposition makes it possible to calculate the variation in stress as a function of coating thickness [28].

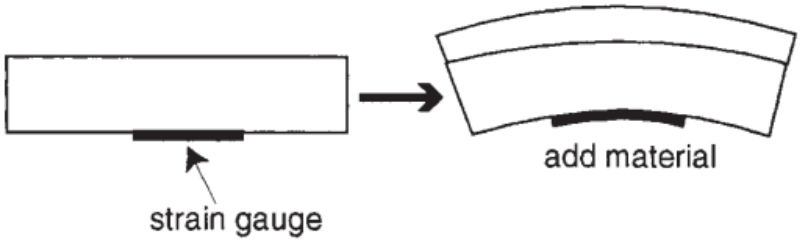

Fig. 3. Change in curvature after coatings deposition [28].

1.3.2. Non-destructive Methods

1.3.2.1. X-ray Diffraction

Using X-ray diffraction is considered as a precise method for measurement of residual stress in materials. The XRD technique has the capability to accurately measure the micro and macro residual stresses using non-destructive method. Any mechanical or electro discharge machining could induce residual stress in the surface. Therefore, such aggressive methods of material removal should be avoided. For the incremental depth profile, layer removal by electropolishing or chemical attack is recommended. Electropolishing method involves the removal of surface layers by submerging the sample into a tank containing a mixture of acids that are saturated with metal salts. A voltage is applied across the sample and tank (anode and cathode respectively) in a way that current flows through for a set of time. This results in the removal of certain amount of material according to the Faraday's first law [21]. Due to the low penetration of the X-ray beams, measurement of very deep or core of thick coatings is not preferred using XRD method which is one limitation of measurement of residual stress using this technique.

Crystal lattice spacing may change due to the strain exerted by formation of residual stress in the materials. Under the tension or compression, the distance between crystallographic planes changes compared to unstressed ones. A schematic of changes crystal spacing under tension is shown in Fig. 4.

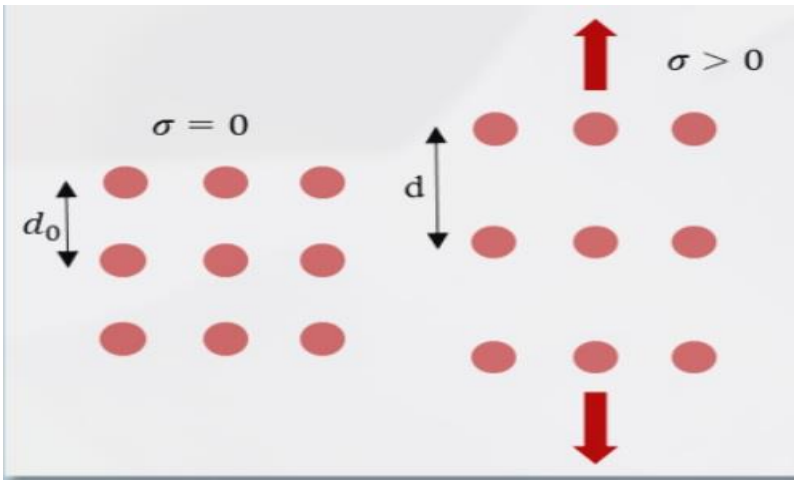

Fig. 4. Schematic of crystal spacing for un-stressed and tensional stressed material [19].

As mentioned before, the deformation due to existence of the residual stresses may cause some micro strains. The shift of diffraction peaks to new position can be used for measurement of residual stress in the samples using the Bragg's equation.

$$n\lambda = 2d \sin \theta \quad (1)$$

where, n is number of wavelengths

λ is the wavelength of x-ray beam

d is the crystal spacing in crystallographic planes

θ is the angular position of diffraction peaks.

1.3.2.2. Neutron Diffraction

Neutron diffraction method, a non-destructive method is used to determine the residual stress in a crystalline material. Neutron diffraction measures strain components from the change in lattice spacing of crystalline material. A pulsed beam of neutron is incident with wide range of energy and small fraction of the rays are deflected into the detectors, located at an angle of 90 degree. The wavelength, λ, of the detected neutrons is calculated using the flight-of-time, t, between the moderator and detector.

$$\lambda = \frac{h}{mL}t \quad (2)$$

where, h is the Planck constant

m is the neutron mass and

L is the neutron flight path from the moderator to the detector.

The angle at which any peak occurs is calculated using the Bragg's equation in equation (2).

When there is strain in the specimen, the lattice spacing changes. Any elastic strain will cause the apparent shift of the diffraction peaks in the value of 2θ for particular reflecting plane illuminated by a fixed wavelength. By differentiating the Bragg's equation,

$$\Delta\theta = -(\Delta d/d_0)\tan\theta_0 \quad (3)$$

where Δd is the change in lattice spacing and,

d_0 is the lattice spacing of a stress-free sample of the material.

Therefore, the strain in the plane can be calculated as:

$$\varepsilon = (\Delta d/d_0) = -\Delta\theta \cot\theta_0 \quad (4)$$

The strain measured is along the scattering vector and is perpendicular to the diffracting planes [29-31].

2. THERMAL SPRAYING TECHNIQUES

Thermal spraying is a generic term given to the group of various deposition methods of protective coatings. Thermal spray coatings follow the process of depositing the coatings by the means of special device or system through which the molten spray particles are thrust into the substrate. Coatings deposited by thermal spraying are mainly finding its application in the aerospace, automobiles, marine, and various protective coatings layer to prevent from corrosion and oxidation.

Thermal spraying process improves the service life and mechanical properties of substrate or whole component with the application of protective coating layers. Not only metals but a wide range of materials such as ceramics, alloys, some polymers can be deposited using thermal spraying techniques. Thermal spraying process is grouped into three major categories: flame spray, electric arc spray and plasma arc spray. These energy sources are used to heat the coating materials either in wire or powder form, to a molten or semi-molten state. The resultant molten particles are then accelerated towards the substrate that are prepared by process gas. Upon impact, mechanical or metallurgical bond formation occurs between the molten particles and the substrate and the high cooling rate aids on solidification of particles which leads to the adhering of the coatings to the substrate. And similarly, the coatings build up in the surface. The Fig. 5 shows the step-by-step deposition process.

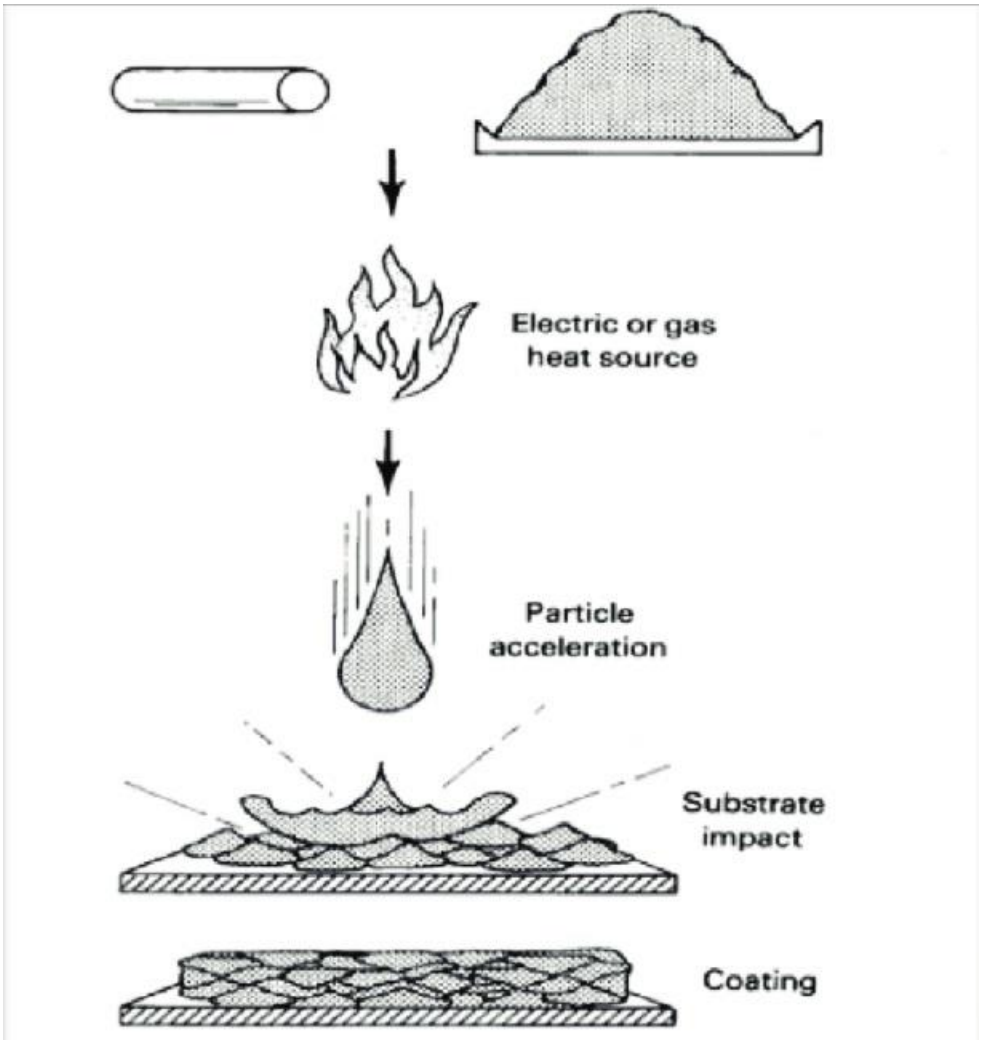

Fig. 5. Thermal spraying deposition process [32].

Wire arc spray, high velocity oxygen fuel (HVOF), plasma spray, cold spray, selective laser melting (SLM) are some commonly used thermal spraying techniques. Among various deposition techniques, cold spray has some advantages that are discussed in next section. Fig. 6 shows various thermal spraying methods in terms of gas temperature and particle velocity during the deposition.

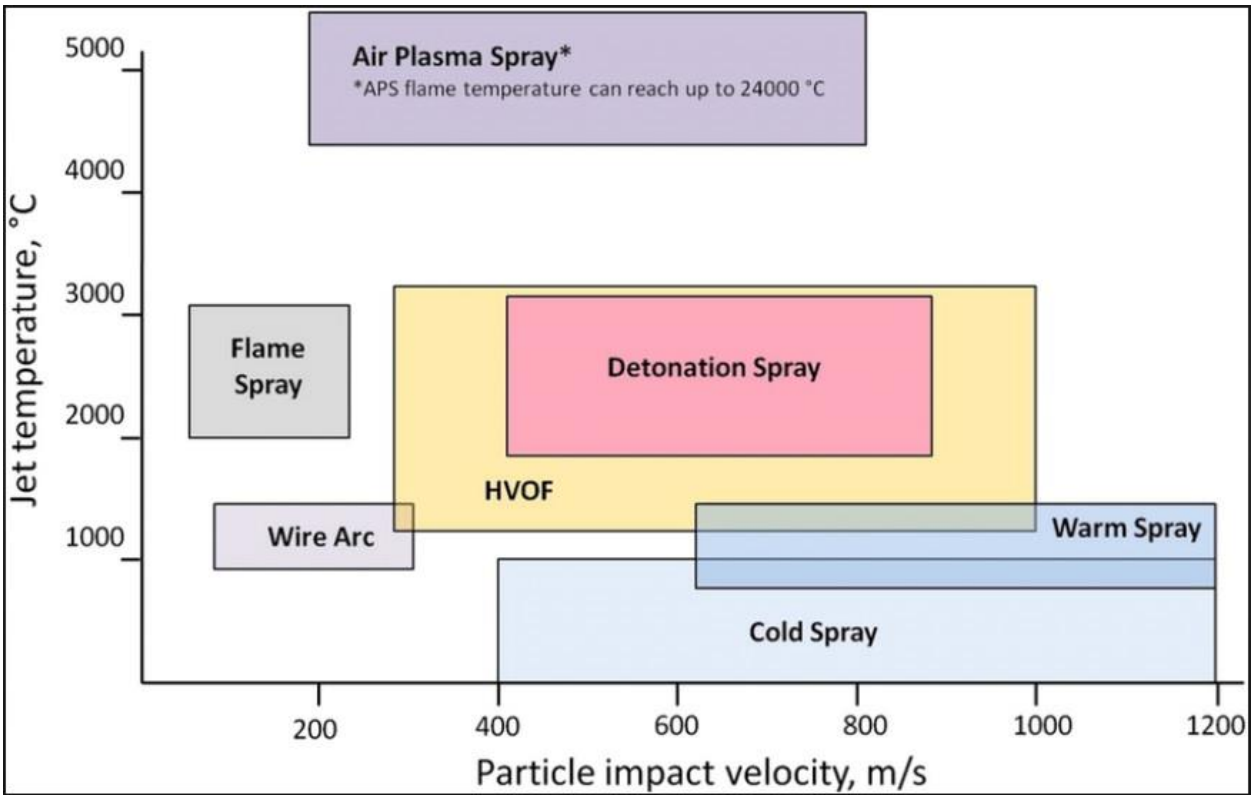

Fig. 6. Gas temperature vs particle velocity for common thermal spray techniques [33].

Various studies have been done to measure the residual stress produced by thermal spray techniques. X. Wang *et al.* [43] has investigated the effect of stress reliving heat treatment on the microstructure and residual stress of Inconel 718. Inconel 718 was fabricated by the laser metal powder bed fusion additive manufacturing process. Micro-indentation tests were done on the stress relieved heat-treated samples and as-fabricated samples. Residual stress of as fabricated samples was found compressive in nature which was relieved after the stress relief heat treatment. After stress relieved heat treatment, the microstructure was relatively homogeneous, and the microhardness value of the sample was increased. Chen *et al.* [35], studied the thermal effect on residual stress of broached Inconel 718 and found it followed the stress profile of tensile at the top surface, gradually changing to compressive at the subsurface. Heat treatment at 550° C for 30 hours resulted in relief of residual stress to almost zero, and after 3000 hours the residual stress

became compressive in nature. Wu and Jiang [36] have studied the effect of thermal relaxation on residual stress and microstructural changes of dual shot-peened Inconel 625 and have found the dependency of the relaxation rate on annealing time and temperature. Dual shot-peening have resulted on high compressive residual stress on the top surface that was relaxed after various isothermal temperatures. High compressive residual stress (-837 MPa) was relaxed up to -487 MPa, and -178 MPa and was stable at elevated temperatures of 500, 600 and 700°C, respectively after the first 15 minutes. Lyphout *et al.* [37], have investigated the residual stress in thick high velocity oxygen-fuel (HVOF) deposited Inconel 718 coatings via various measuring methods. Successive tensile and compressive residual stress was observed throughout the coatings and compressive residual stress at the interface which could have been the reason for the strong bonding of the coatings. Moreover, increasing coating thickness does not seem to have effect on the residual stress behavior through the coatings, but the difference in stress amplitude at the interface seems to decrease significantly with increased coating thickness. Wang *et al.* [38], have studied the residual stress evolution in laser melted powder bed fusion and found compressive residual stress that was relieved after heat treatment. After heat treatment, the microstructure was homogenized resulting the increased hardness and the residual stress was relieved significantly. Kim *et al*. [39], have studied the effect of low temperature heat treatment (100-400°C) on cold sprayed Inconel 718. Compressive residual stress was found on the Inconel 718 and low temperature heat treatment resulted in residual stress relaxation, whereas increased temperature resulted on opposite. The residual stress at low temperature was relieved and at high temperature of 400°C, residual stress was increased. Singh *et al.* [40] have investigated the residual stress with increasing coating thickness and found that the adhesion strength of the cold sprayed Inconel 718 was reduced with the coating thickness resulting in the failure of coatings. Residual stress was

measured at four different thickness of the coatings and was decreased with increasing coating thickness. The adhesion test of the coatings was conducted for each successive coating layers and the adhesion strength of the coating decreased with the increasing coating thickness. The coating was delaminated and peeled off from the substrate after the coating thickness reached above approximately 500μm. Lihong Wu, *et al.* [41] have studied the effect of thermal relaxation on residual stress and microstructural change of dual shot peened Inconel 625. Sample of 20mm × 15mm × 5mm was prepared by dual shot peening, first by cast steel balls and second by ceramic balls. High compressive residual stress was observed on the top surface of the dual shot peened sample which was relaxed after various isothermal temperatures. High compressive residual stress (-837 MPa) was relaxed up to -487MPa, -332MPa and -178MPa and were stable at elevated temperatures of 500°C, 600°C and 700°C respectively at first 15 minutes. Relaxation rate increased with the annealing time and was dependent on the temperatures. Residual stress after an hour of isothermal treatment was analyzed and high compressive residual stress was retained at the sub-surface layers.

I. van Zyl, *et al*. [42] have investigated the residual stresses in the titanium alloy samples produced by direct metal laser sintering (DLMS). Residual stress along the different layers (10-40 layers) varied significantly with vertical location. Samples of 1×1 cm cube was prepared with and without support by DMLS and residual stress was measured on the middle of the top surface. Residual stress on the top surface of the sample of both samples (e.g., with and without support) were tensile and was similar to the mean residual stress received from the different layers. Sample with the support should be heat-treated before detaching to avoid deformations. The direction of major residual stress in Ti-6Al-4V alloy was coaxial with the scanning direction. Robinson *et al.* [43] have analyzed residual stress in the SLM prepared titanium alloy. Single melt pool and

multiple melt pool SLM prepared samples were investigated for residual stress. The residual stress in the material after the grit-blasting and prior to laser treatment was measured and was tensile in nature. Single melt pool was examined for residual stress using XRD method. The stress in the mid portion of the single melt pool was tensile in nature while the edges were in compression. Mishurova *et al*. [44] has investigated the residual stress of Ti-6Al-4V samples on different conditions i.e., as built-in base plate, released from base plate and heat treated on base plate. The samples were manufactured additively by selective laser melting (SLM) under different scanning velocities to compare the residual stress state on different energy densities. Four bridge shaped samples were prepared with different energy density values. Residual stress profile with higher energy density showed similar profile for the samples with base plate and released from base plate whereas the residual stress profile showed slight broadening of high strain region for samples with low energy density. The heat-treated samples showed decreased residual stress value of almost zero. All samples showed linear increase of stress with depth up to the maximum around 70μm depth. W. Rae *et al.* [45], has studied the effect of stress relaxation heat treatment on residual stress of Ti-6Al-4V. The stress relaxation testing was conducted to the specimen under isothermal conditions between 500-750° Celsius at interval of 50°C. Almost 50% reduction in stress was noted after one hour heat treatment at 500° C. With increasing temperature, there was 65% to 90% reduction in stress between 600 and 650° C respectively. There was complete stress relaxation after 30 minutes at both 700 and 750°C. There has been several research in Ti-6Al-4V produced by different thermal spray process. However, we can find hardly any literatures for cold sprayed samples.

Residual stress can be either tensile or compressive in nature. In general, residual stress induced by machining are tensile followed by compressive residual stress underneath the surface.

3. COLD SPRAYING

Cold Spraying (CS), also known as Cold Gas Dynamic Spray Process (CGDS) was originally developed by chance and patented by Dr. Anatolii N. Papyrin and his colleagues in Russian Academic of Sciences [46].

CS is considered a relatively new deposition technique that uses conversing-diverging nozzle at a very high supersonic velocity. This is the only thermal spray technology that sprays feedstock powder in solid-state condition unlike other thermal spraying technologies. It uses a gas to accelerate the powder particles at supersonic velocity. The powders are accelerated towards the substrate where they deform plastically upon impact and impinge, and bond to each other by mechanical interlock. The process temperature is always below the melting temperature of the powder particles that are to be bombarded. Hence the name cold spray. This deformation will result in the adhesion of the coating layers to each other and their adhesion to the substrate. Schematic a CS system is shown in Fig. 7. The cold spray system usually comprises of following:

- Powder feeder
- Gas heater
- Propellant gas
- Nozzle
- Spraying chamber

Compressed inert gas (helium/nitrogen) is heated to temperatures generally in the range of (300-800℃). Unlike the traditional thermal spray process, the gas is not heated to melt the powder particles. However, the gas is heated to increase the sonic velocity. This heated gas is then passed through the converging-diverging nozzle to create a supersonic gas velocity. The powder stream is injected at the nozzle prior to the throat where the gas has expanded at low pressure.

The venturi effect in the converging-diverging nozzle creates the high supersonic velocity. High velocity is achieved at the expansion area of the nozzle where certain pressure drop is also observed and recorded. The velocity gained being more than the critical velocity, the powder particles impact on the substrate and are adhered to the substrate due to plastic deformation. Following layers of coatings are deposited subsequently.

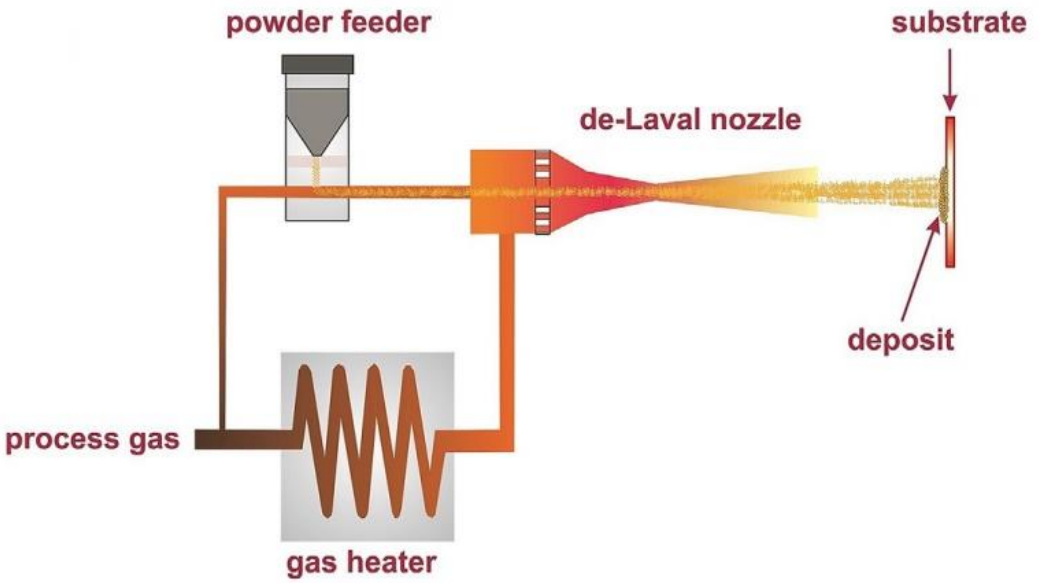

Fig. 7. Schematic of CS system [47].

The coatings deposited by CS technology has several advantages over other thermal spray technologies [48]. Some are listed below:

High density: In CS, the powder particles with the velocity greater than critical velocities are only plastically deformed and deposited. Every sprayed particle shot peens the underlying layer and are plastically deformed, thereby increasing the density.

Minimum thermal input to substrate: In traditional thermal spray process, the substrate is heated prior to deposition and the sprayed powder particles are completely or partially melted. This will make difficult to process the temperature sensitive materials such as magnesium, etc. In

addition, temperature-induced warping of the substrate is also a concern when the thickness of the specimen is small. However, cold spray could be used to repair parts and components made of temperature sensitive materials.

High bond strength: Cold sprayed coatings exhibit very high bond strength followed plastic deformation of the particles including metals such as aluminum, titanium, nickel, etc.

Thick coatings: CS can produce the coatings layer up to the thickness of 4 mm. Since the CS coatings is generally compressive in nature, thick layers could be deposited over many substrates without any bond failure.

No phase change: As CS does not use high temperature, the powder particles are not melted and there is no risk of resulting oxidation, formation of metastable phases, preferential loss of some constituent, etc.

No oxidation: The risk of oxidation during the thermal spray processing of oxygen-sensitive materials such as aluminum, copper, magnesium, and their alloys persists as increasing the temperature exponentially accelerates the oxidation. However, CS does not heat the material to a very high temperature and uses inert gas, which effectively shields the spalts that are formed over the substrate. Hence, the oxidation in CS is almost completely avoided.

High corrosion resistance: Above mentioned advantages, high density, phase purity and homogeneous microstructure combined yield excellent corrosion resistance characteristics.

The coatings deposited using CS technology present less oxidation and thermally induced stresses due to lower temperature of the sprayed solid particles. However, the high velocity impact and deformation of particles may result in residual stress build-up in the CS deposited coatings. To this end, investigation on residual stress formation in CS deposited coatings is important to understand the thermo-mechanical behavior of the coatings during service condition.

The quality of the sprayed coatings depends upon various parameters. Some of the critical parameters are discussed below:

Particle velocity and temperature: The cold spray process involves the preheating of the main gas flow and combining with the particle gas mixture from the high-pressure powder feeder into the mixing chamber. The temperature used in cold spray deposition is below the melting point of the feedstock powder. Hence the cold spray deposition is the solid-state deposition attributed to the plastic deformation. The conversion of the kinetic energy into the mechanical and thermal energy occurs when the particles impact the substrate with a very high velocity. Particle velocity is influenced by several factors such as gas temperature, weight of the main gas, pressure, etc. Normally, nitrogen or helium are the two gases used in cold spray. The particle velocity is dependent on both the gas temperature as well as the molecular weight of the gas.

$$\nu = \left(\frac{\gamma RT}{M_w}\right)^{1/2} \tag{5}$$

where,

ν is the velocity of particle.

γ is the ratio of the specific heats (1.4 for air and 1.66 for He)

R is the gas constant (8.314 J/mole K)

T is the gas temperature in K

M_w is the molecular weight of the gas.

Nozzle Design: One of the main characteristics of the cold spray is high speed gas jet. Supersonic flows in gas dynamics are obtained by using a convergent-divergent nozzle. The throat diameter and the exit divergence play a very important role in the deposition.

Standoff distance: Several factors determine the standoff distance such as particle size, density, shockwave. Particle size is one of the factors that plays an important role in the high

velocity achievement and standoff distance. Generally, the particle size of 5-100 microns is used in the cold spray. Several studies has been performed [49] to study the effect of standoff distance on various properties of cold-sprayed coatings. It is observed that the deposition efficiency decreased with the increase of standoff distance ranging from 10mm to 110mm.

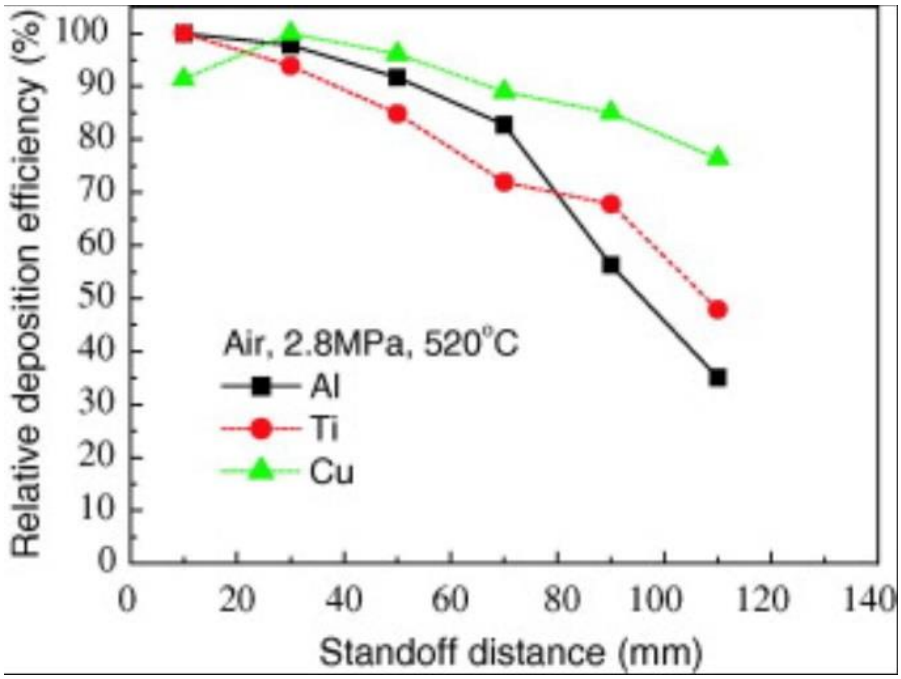

Fig. 8. Effect on deposition efficiencies if Al, Ti and Cu powders with standoff distance [49]

3.1. Significance and Objectives of this Study

In the present study, residual stresses induced by the CS process in well-known industrial metal alloys were evaluated by x-ray diffraction. The effects of heat treatment on residual stresses in three types of coatings were also studied here. The residual stress induced by the CS deposition technique and the effect of heat treatment performed at a range of temperature on residual stress were previously studied [35,36,50]. However, this work pays special attention to the porosity formation and its relationship with residual stress content of cold sprayed metallic alloys. We have tried to investigate the effect of heat treatment on residual stress based on porosity annihilation due to application of heat treatment in all samples. This is also studied in terms of crack

propagation before and after heat treatment in the coating microstructures. This study was successful in Inconel samples, but no apparent crack annihilation was observed after stress relaxation heat treatment in Ti-6Al-4V samples. To this end, wear test was performed on CS deposited titanium alloy samples to correlate wear resistance of the samples to residual stress content before and after heat treatment. The results from this study will contribute to better understanding the performance of cold spray deposited superalloys under service conditions and the effect of stress relaxation heat treatment on elimination of residual stress.

4. EXPERIMENTAL PROCEDURE

4.1. Materials

Commercially available grade powder PG-AMP-1060 with particle size 45-90 μm and PG-AMP-1070 with particle size 10-32 μm have been used for deposition of Inconel 625, and Inconel 718, respectively. Ti-6Al-4V powders, commercially known as PG-AMP-1120 with particle size of 15-45 μm was used for deposition of coating on aluminum substrate in this study. With respective particle sizes, it is clear from the images that all powder particles have round, spherical shape as observed in the SEM micrographs of the feedstock powders of Inconel 625, Inconel 718 and Ti-6Al-4V shown in Fig. 9 The powder particles have exhibited relatively similar size distribution and exhibit round morphology.

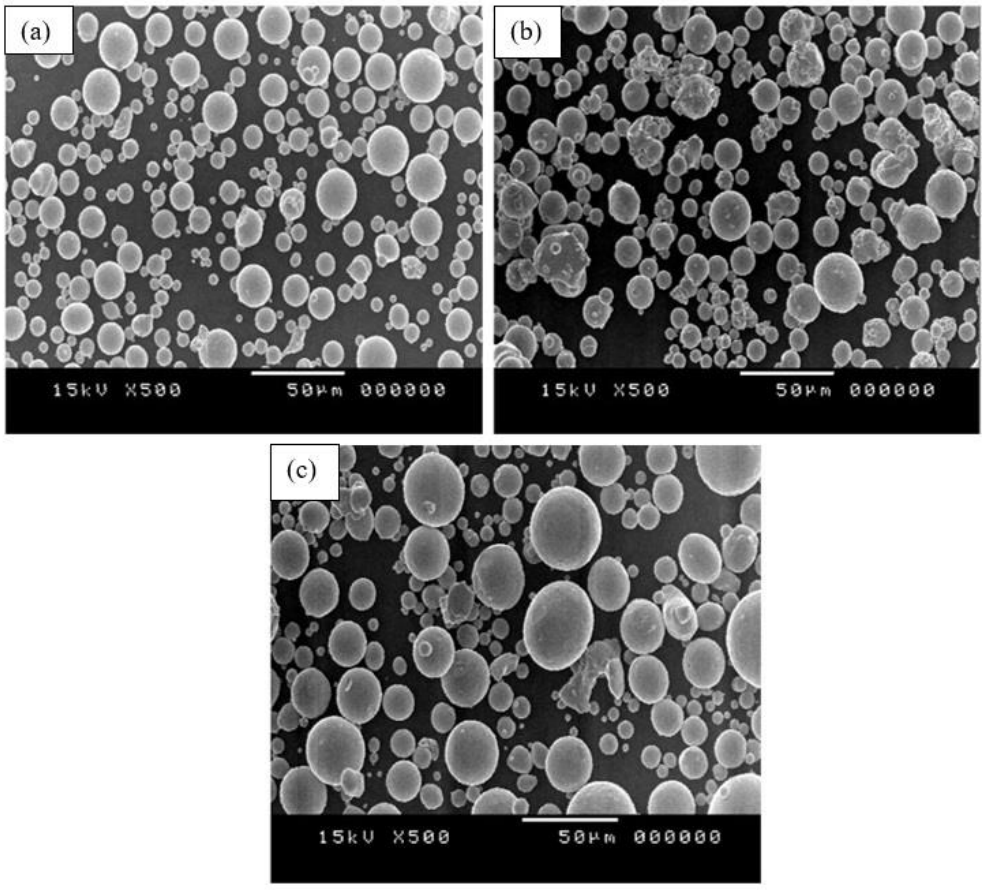

Fig. 9. SEM micrographs of feedstock powder (a) Inconel 625, (b) Inconel 718, and (c) Ti-6Al-4V [57].

The chemical composition of the powders of Inconel 625, Inconel 718, and Ti-6Al-4V is listed in the Table 1.

Table 1. Chemical composition of Inconel 625, Inconel 718, Ti-6Al-4V.

Element	Ni	Cr	Ti	Al	V	Nb	Fe	Mo	Nb+Ta	Sn	Si	O
Inconel 625 (wt., %)	Bal	22	-	-	-	-	2	9.4	4.8	-	-	-
Inconel 718 (wt., %)	52.5	19.0	-	0.5	-	5.2	18.8	3.1	-	-	-	-
Ti-6Al-4V (wt., %)	< 0.02	< 0.01	Bal	6.48	4.03	-	0.17	-	-	0.02	0.01	0.17

4.2. Coating Deposition

A PCS1000 high pressure cold spray system by Plasma Giken (Saitama, Japan) was used for deposition of all coating samples. The process parameters of the cold spraying used in this study are listed in the Table 2.

Table 2. Process parameter for cold spraying.

Process Parameters	Inconel 718& 625	Ti-6Al-4V
Spray Distance (mm)	300	330
Feed rate (rpm)	2.4	2.5
Current (A)	550	550
Voltage (V)	33	35
Pressure (MPa)	7	7
Primary Gas	Nitrogen	Nitrogen
Temperature (°C)	1000	1100

4.3. Microstructural Characterization

All as sprayed and heat-treated coating samples were cut and mounted with epoxy resin. The samples underwent grinding, polishing, and etching before the microstructural observation according to ASTM E407-07 (2015) [51]. To investigate microstructural features, the cross section of the etched section was examined using Digital Microscope, VHX-7000 (Keyence corporation

of America, 500 Park Boulevard, Itasca, IL 60143, U.S.A). Microstructural characterization of the samples at high magnification was performed using JEOL JSM-6490 LV Scanning Electron Microscopy (SEM) (JEOL USA, Peabody, MN) and the porosity of the samples were measured by the image analysis method. SEM is a type of equipment that uses an electron beam instead of light to magnify the image. Based on the five micrographs taken at five different locations on each sample, the apparent porosity of coatings was determined according to ASTM E 2109-00 [52] using image analysis.

4.4. Stress Relief Heat Treatment

During the CS, the high velocity impact could induce compressive residual stress and create dislocation tangles associated with plastic deformation of the powder particles. To better understand the effect of heat treatment on residual stress in cold sprayed samples, stress relief heat treatment was performed on each sample according to standard [53]. Stress relief heat treatment were performed to enhance the cohesion between the lamella by increasing diffusion across the atoms, and elimination of fine pores within the microstructure. It is expected to reduce the residual stress induced by high-velocity impact of solid particles during the cold spraying process. For stress relief heat treatment, furnace as shown in Fig. 10 was used and the optimum heat treatment temperature for each material was found in available literatures [53-55]. Table 3 lists the condition for stress relief heat treatment in this study. At first, the furnace was heated up to the set temperature for Inconel 625 and Inconel 718 i.e., 800℃. Both nickel-based samples were placed on the furnace at 800℃. and held for one hour, the sample was then air cooled. To perform the stress relief heat treatment on Ti-6Al-4V, the furnace was first heated up to 650℃. The Ti-6AL-4V sample was then placed on the heated furnace and held for one hour, the sample was then air cooled.

Table 3. Heat treatment temperatures for various samples.

Alloys	Heat Treatment Temperature (°C)	Time (Hour)	Cooling method
Inconel 625	800	1	Air Cooled
Inconel 718	800	1	Air Cooled
Ti-6Al-4V	650	1	Air Cooled

The furnace as shown in Fig. 10 was used for the heat treatment process in this study.

Fig. 10. The furnace used for heat treatment after CS deposition in this study.

4.5. Residual Stress Measurement

Residual stress of the cold sprayed samples was measured by X-ray diffraction method. Residual stress measurement was performed using an XStress 3000 G2R-F (Stresstech, PA, USA) X-ray diffractometer equipped with a type HPC detector. For Inconel 718 and Inconel 625, the radiation used was Mn-Kα, giving the 2θ position of 153.5°. The peak position was determined at sixteen different Ψ tilts (2×0, ± 15.5, ± 22.2, ± 27.6, ± 32.2, ± 36.7, ± 40.9, ± 45). Bulk elastic constant, $E = 205\ GPa$ and $\nu = 0.386$. For Ti-6Al-4V, the radiation used was Cu-kα, giving the 2θ position of 140.5°. The peak position was determined at twelve different Ψ tilts (2×0, ± 17.4,

$\pm$ 25, $\pm$ 31.2, $\pm$ 36.8, $\pm$ 42). Bulk elastic constant, $E = 114\ GPa$ and $\nu = 0.342$. The stress values were obtained by converting the strain using the bulk elastic constant and poisons ratio. For the residual stress calculation, "$\sin^2 \Psi$" method at different tilt angles was used. The operational process parameter used for the residual stress measurement before and after heat treatment are listed in the Table 4.

Table 4. Process parameter and technical features to measure the residual stress before and after heat treatment.

Parameter	**(Inconel 625)**	**(Inconel 718)**	**(Ti-6Al-4V)**
Detector Geometry	Modified X	Modified X	Modified X
Detector Type	HPC, direct detect	HPC, direct detect	HPC, direct detect
Tube Power	30 kV x 6.6mA, 100%	30 kV x 6.6mA, 100%	30 kV x 6.6mA, 100%
Collimator Size (mm Ø)	1	1	1
Radiation	Mn-Kα	Mn-Kα	Cu-Kα (Ti-Kα)*
Wavelength λ (Å)	2.10	2.10	1.54
Exposure Time (s)	10 (25-35)*	10 (25-35)*	30 (10)*
Diffraction Plane	311	311	213 (110) *
Bragg's Angle	153.5 (152-153)*	153.5 (152-153)*	140.5 (137.5)*
Penetration Depth (μm)	4.2 (6-7)*	4.2 (6-7)*	5.2 (8.3)*

*For the measurement of heat-treated sample.

Residual stress measurements were performed along transverse (perpendicular to spray direction) i.e. 90°, longitudinal (spray direction) i.e. 0° and 45° at the surface and at depth of approximately 1mm for each sample as shown in Fig. 11.

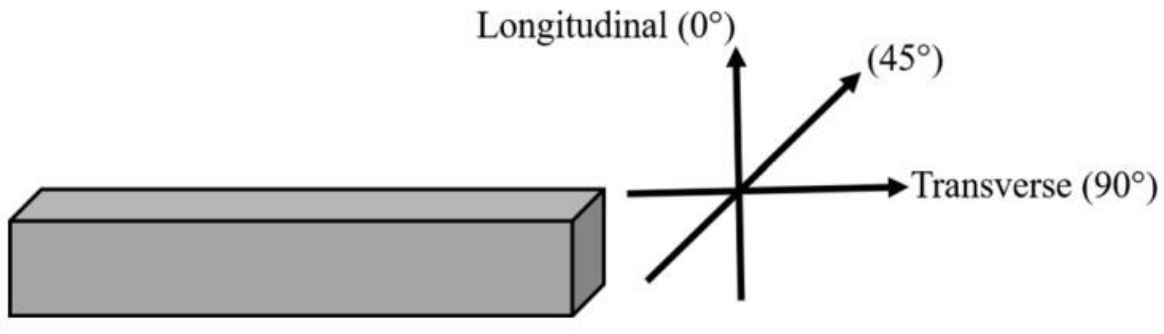

Fig. 11. Schematic diagram showing the direction of residual stress measurements.

Electropolishing technique was performed to determine the residual stress at the sub-surface. Samples of Inconel 625, Inconel 718 and Ti-6Al-4V after residual stress measurement using X-ray diffraction method are shown in Fig. 12 (a), (b) and (c), respectively.

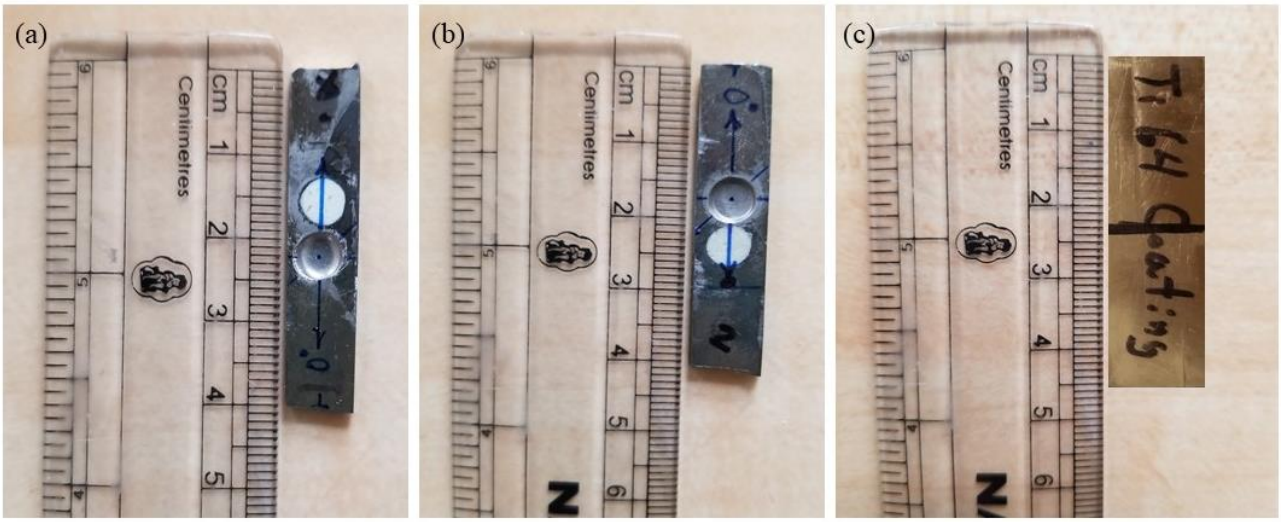

Fig. 12. (a) Inconel 625, (b) Inconel 718, and (c) Ti6Al-4V samples subjected to x-ray diffraction measurement of residual stress.

4.6. Micro-indentation Test

Indentation techniques are commonly used to measure the resistance of the materials to deform under certain applied load. Vickers micro-indentation is one of the most commonly used and popular method for hardness measurement. Vickers micro-indentation method was used in this study. The test was performed on all samples for the hardness measurement before and after the heat treatment using a Micromet 5140, Buhler, USA. Micro indentation tests were performed at minimum of eleven random points on each sample before and after heat treatment according to ASTM E92-17 [56]. For Inconel alloy and titanium alloy, Vickers hardness test was performed at the applied load of 100 gf for 15 seconds for all metallic samples in this study.

4.7. Crack Formation

In order to investigate the crack formation in the as sprayed and heat-treated samples, Vickers micro-indentation was performed. Several indents were made on the sample with the applied load of 100gf for 15 seconds. With the force applied and the presence of residual stress, porosity, cracks could be induced on the surface of the material. The indents and cracks developed around is then observed by using Digital Microscope, VHX-7000 (Keyence corporation of America, 500 Park Boulevard, Itasca, IL 60143, U.S.A).

4.8. Dry Sliding Wear Test

Wear resistant behavior of CS deposited Ti-6Al-4V sample before and after heat treatment were measured in this study. Tests were carried out with a Micro tribometer, UMT 2MO machine (Bruker, USA) using the dry pin-on-disk contact geometry. The test parameters used for the experiment is listed in Table 5 according to ASTM G99-17 [64].

Table 5. Test parameters used for the pin-on-disc wear test on CS deposited Ti-6Al-4V samples.

Parameters	**Values**
Normal Force (N)	1
Sliding Speed (rpm)	280
Sliding Distance (m)	105.557
Pin-end Diameter, spherical (mm)	2
Environment	air
Temperature, nominal (°C)	23

5. RESULTS AND DISCUSSIONS

5.1. Microstructural Observation

The microstructural characteristics and the properties of cold sprayed coatings greatly depends on the size distribution of the feedstock powders used for deposition process. The nominal composition and particle geometry is reported by the powder manufacturer as listed in Table 1.

Fig. 13 (a) shows the micrographs of as sprayed Inconel 625. The micrograph shows the presence of relatively dense deposit build-up with a porosity level of 1.67±0.45 Area % according to image analysis. Pores and cracks are round and elongated in shape. The measured porosity levels of Inconel 625 are found to be 0.95±0.33 Area % after heat treatment as shown in Fig. 13 (b).

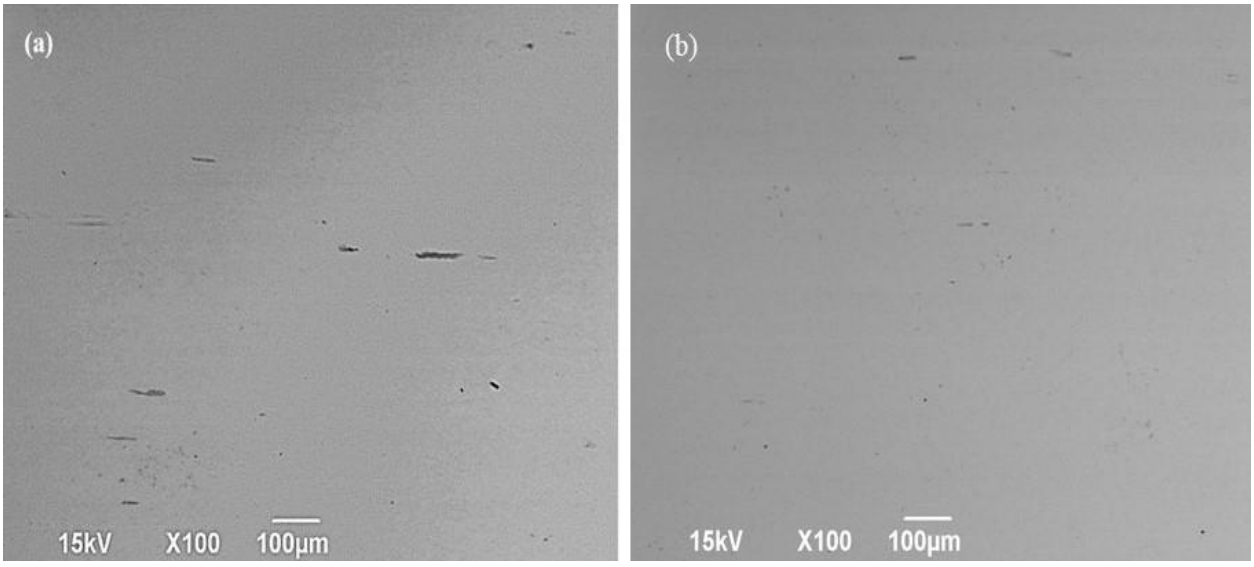

Fig. 13. SEM micrographs of the cross-sectional regions of cold spray deposited Inconel 625 (a) as sprayed, and (b) heat-treated samples.

Compared to Inconel 625, Inconel 718 has a higher porosity level of 4.39±0.55 Area % and the voids and cracks are mostly in round shape as shown in Fig. 14 (a). The porosity level after the heat treatment of Inconel 718 was found to be 2.35±0.40 Area % as shown in Fig. 14 (b). Heat treatment accelerates the diffusion of atoms within the microstructure leading to the elimination of very small pores and overall reduction in pore size [58]. Moreover, elevated temperatures may

lead to the consolidation of inter-particle boundaries, which can result in the shrinkage of voids. The results of porosity reduction in this study are in good agreement with the results reported in literature [59] for heat-treated nickel-based alloys.

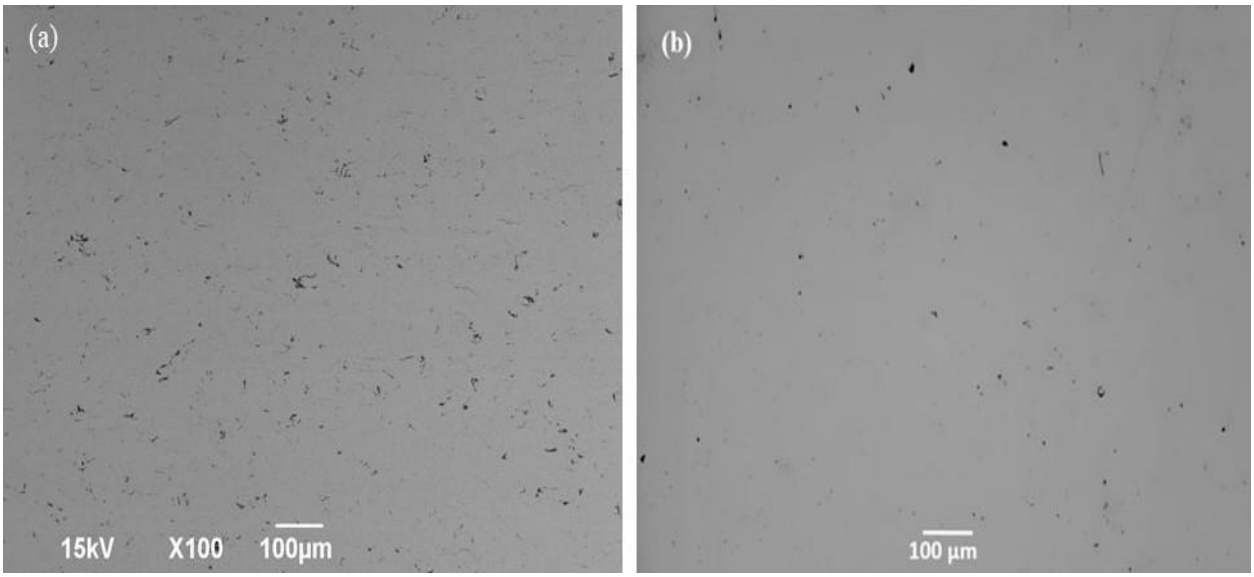

Fig. 14. SEM micrographs of the cross-sectional regions of Inconel 718 deposited by cold spraying (a) as sprayed, and (b) heat-treated samples.

Microstructure of Ti-6Al-4V exhibit higher level of porosity compared to both nickel-based superalloys studied here as shown in Fig. 15 (a). CS deposited titanium alloy, being a very porous material, exhibited large number of pores compared to Inconel 625 and Inconel 718. The measured porosity level for as sprayed Ti-6Al-4V was found to be 8.28±0.17 Area %. The voids are irregular in shape and size and distributed uniformly within the microstructure of the coating. After heat treatment, the porosity level was significantly decreased to 3.89±0.16 Area % as shown in Fig. 15 (b).

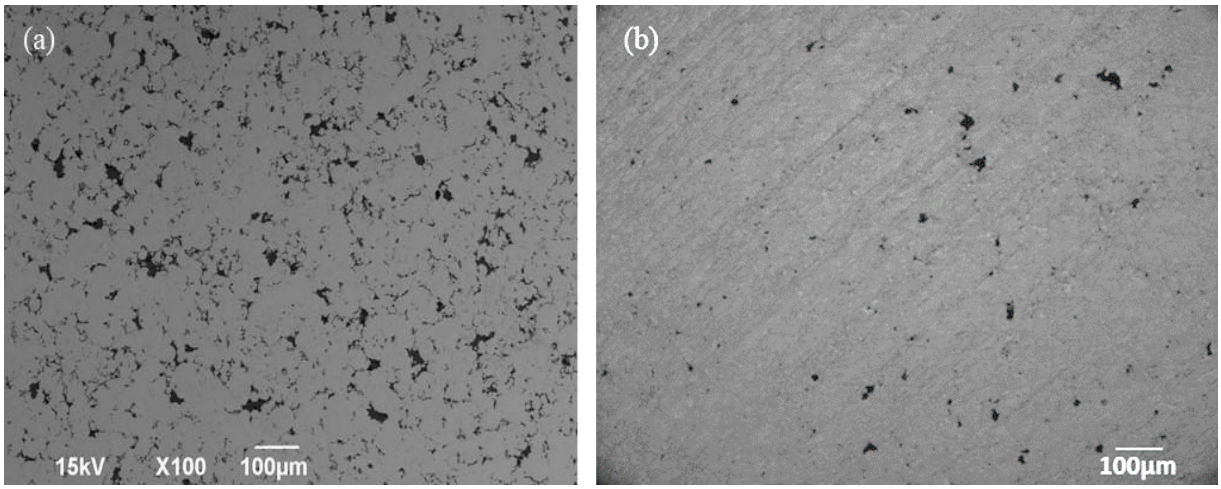

Fig. 15. SEM micrographs of the cross-sectional regions of (a) as-sprayed Ti-6Al-4V, and (b) heat-treated Ti-6Al-4V deposited by cold spraying.

5.2. Residual Stress

In this section, results of residual stress measurements as explained in previous section for cold sprayed Inconel 625, Inconel 718, and Ti-6Al-4V is presented. Stress state at the free (top) surface of samples could be altered due to various surface treatment processes such as grinding, polishing, and machining. Therefore, the residual stress state at the sub-surface is more important and of major concern to be investigated in CS deposited cold spraying samples in this study.

5.2.1. Residual Stress in Inconel 625

Residual stress at the surface and sub-surface were measured before and after the heat treatment process as shown in Fig. 16. The measurement results showed that the residual stress on the top surface is mostly tensile in nature while at sub-surface it was mostly compressiveIn cold spraying coatings, high velocity impact leads to solid state deposition of powder associated with their severe plastic deformation and impingement. This process develops the compressive force on each layer of deposition thus it is reasonable to form a residual stress with compressive nature within the core of cold spray deposited coatings. L, Wu et al. [41], have found compressive residual stress on shot peened Inconel 718 samples. Our result from CS can be related with the

result from literature as CS causes the plastic deformation of the particles. Peening effect is also one of the factors resulting in compressive residual stress in CS. The measurement on the heat-treated samples indicated that residual stresses were significantly reduced by excretion of stress with opposite sign. As we are dealing with the Type II stress, on micro level, porosities, dislocations, etc., could be influenced by heat treatment. During the heat treatment, the dislocation tangles associated with plastic deformation of particles could be reduced, dissipating the stress of opposite sign. The stress when reacting with the pre-existing residual stress could cause the stress distribution depending upon the magnitude of generated stress during the stress relief heat treatment. Tensile stress was measured on the surface before heat treatment which is significantly reduces changing its stress state to compressive after application of heat treatment on Inconel 625 samples as seen in Fig. 16 (b). Since, surface of the material could be influenced by various surface treatments, residual stress on the core of the sample is considered in this study.

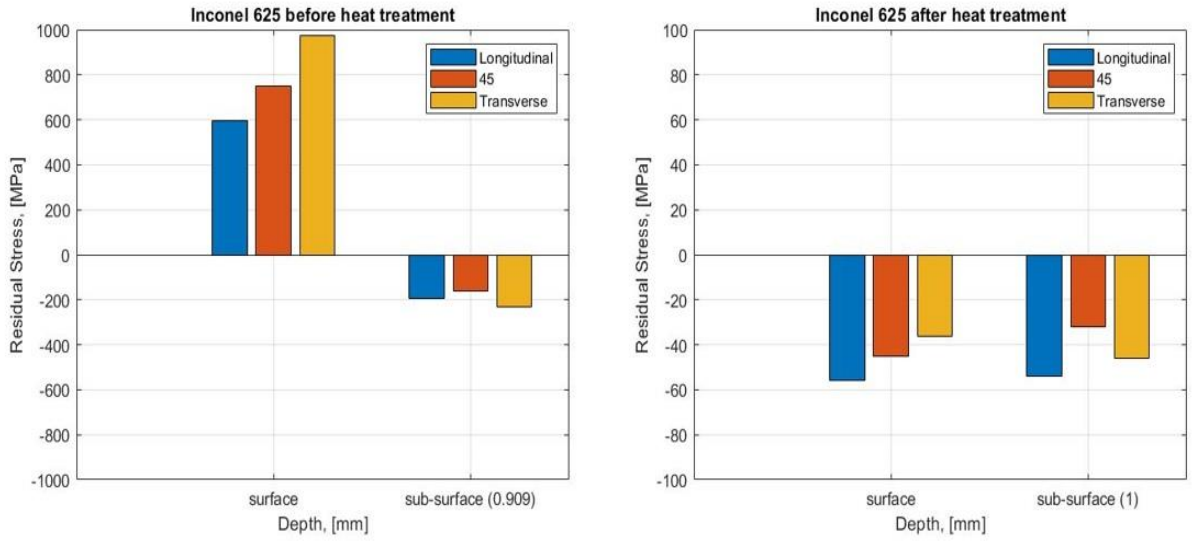

Fig. 16. Residual stress distribution along the longitudinal, 45°, and transverse direction of Inconel 625 (a) as sprayed, and (b) after heat treatment.

5.2.2. Residual Stress in Inconel 718

Residual stress in Inconel 718 is compressive in nature and gradually increasing along the depth as shown in the Fig. 17 (a). Inconel 718 residual stress state follows the assumption of compressive residual stress to be induced during cold spray. Residual stress is found to be maximum along the longitudinal direction (160 MPa) on the surface. After the heat treatment while residual stress was slightly changed on the surface, it was significantly reduced in the sub-surface (1 mm depth) as shown in Fig. 17 (b). The stress profile could vary with the thermal spray deposition. Residual stress exhibited by HVOF and CS could have a compression nature as reported in the literatures [3,8-10,70]. Similar characteristic was found in CS deposited samples studied in this study. The compressive stress is reduced by the stress induced during the heat treatment with the opposite sign. The sign and magnitude of the stress generated during the heat treatment could result in reduction of residual stress after heat treatment. Cooling medium and cooling rate is also another factor that could influence the residual stress on the sample. The samples were air cooled after stress relief heat treatment. The cooling rate at the surface and sub-surface could be different as the surface region is exposed to air directly resulting in higher heat transfer rate. The differences in cooling rate and elimination of porosities which can cause generation of stresses with opposite signs could increase compressive residual stress after heat treatment. Kim et al., [39] studied the effect of low temperature heat treatment and found slight increased compressive state of stress after application of heat treatment. There could be several factors affecting the stress state on the free surface therefore it can exhibit different rate of change in stress compared with core region.

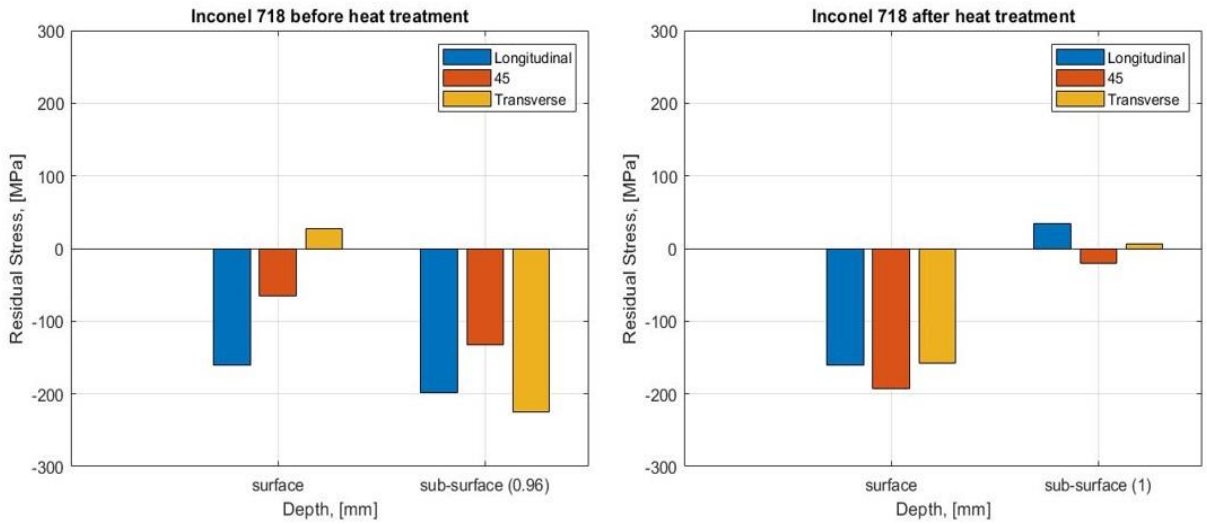

Fig. 17. Residual stress distribution along the longitudinal, 45°, and transverse direction of Inconel 718 (a) as sprayed, and (b) after heat treatment.

5.2.3. Residual Stress in Ti-6Al-4V

Cold sprayed Ti-6Al-4V has also exhibited compressive residual stress in both top surface and approximately 1 mm under surface as shown in Fig. 18 (a). However, residual stress was relieved significantly after heat treatment at 650°C for one-hour as shown in Fig. 18 (b). Tensile residual stress was found on DMLS [43] and SLM [42] processes. D. Boruah et al., [71] have found tensile residual stress exposed by CS in contrast with the results obtained in this study. Higher thermal stress and quenching stress were found to be dominant over the peening stress in CS, which could have resulted in formation of tensile residual stress. However, thermal stress was not significantly higher enough to dominate over the peening effect by CS in our study resulting compressive residual stress as expected. After heat treatment, induced compressive residual stress was significantly relieved as shown in Fig. 18 (b). The sign and magnitude of the stress generated during the heat treatment could act againstthe pre-existing residual stress on the material resulting reduced compressive residual stress.

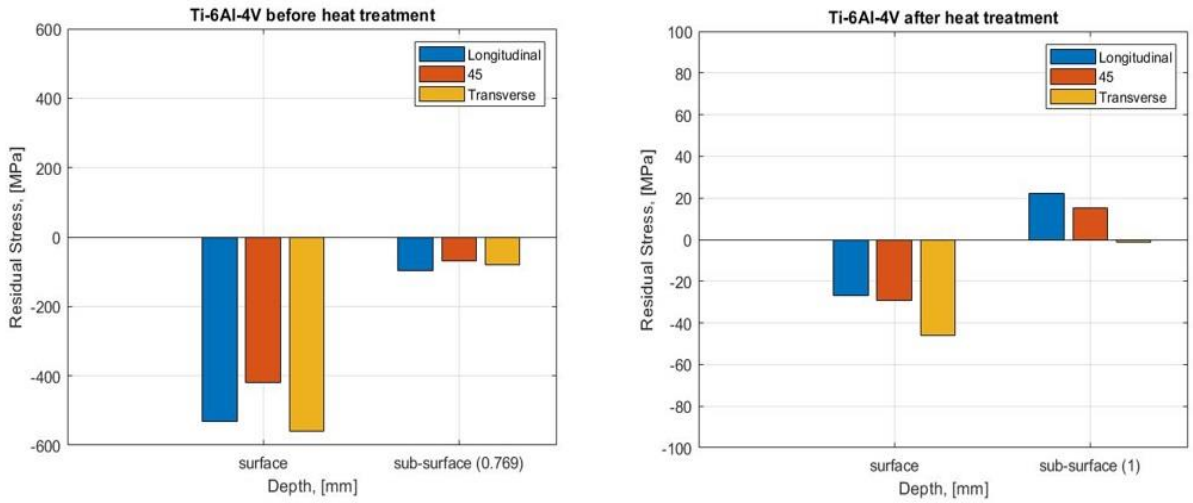

Fig. 18. Residual stress distribution along the longitudinal, 45°, and transverse direction of Ti-6Al-4V (a) as sprayed, and (b) after heat treatment.

5.3. Hardness

The measured hardness value of the as sprayed and heat-treated samples is listed on the Table 6. Inconel 625 exhibits a high-density microstructure with lowest amount of porosity which combined with plastic deformation and strain hardening during cold spraying can result in having highest hardness among all samples in this study. Inconel 718 contained more porosity compared to Inconel 625 and it had lower hardness. The hardness result for as sprayed samples is in good agreement with the literatures provided [60,61]. As mentioned before, Ti-6Al-4V exhibited a very porous microstructure which could be one of the reasons for having the lowest measured hardness among three samples studied here.

A significant reduction of hardness (~%25) occurred in CS deposited Inconel 625 after heat treatment. While the reduction of hardness happened at a very lower rate for Inconel 718 and Ti-6Al-4V (%13 and %16, respectively). While due to the higher rate of pore elimination in Ti-6Al-4V and Inconel 718, it is assumed that this sample may experience higher rate of decrease in hardness after heat treatment. However, the experimental results did not confirm our assumptions

which indicates that the softening of material after stress relaxation heat treatment in addition to pore elimination can depend on other parameters which can be studied separately in the future.

Table 6. Hardness of Inconel 625, Inconel 718 and Ti-6Al-4V before and after heat treatment.

Samples	**Hardness before heat treatment (HV)**	**Hardness after heat treatment (HV)**
Inconel 625	538.16± 32.91	406.54± 38.91
Inconel 718	472.66± 31.42	414.76± 33.42
Ti-6Al-4V	406.79±13.99	344.01±21.61

5.4. Crack Formation

Vickers indentation was performed again on as sprayed and heat-treated samples to observe crack propagation due to the existence of residual stress when samples experience plastic deformation. Fig. 19 & 20 show the indents and cracks formed by micro indentation on both as sprayed and heat-treated Inconel 625 and 718 samples. Residual stress within the sample can significantly affect the crack propagation of the material. Residual stress in terms of crack propagation can also be beneficial or harmful because they affect its ability to sustain the loads. Generally, the residual stress (tensile residual stress) support or work against (compressive residual stress) the penetration of the material by the indenter. Tensile residual stress increases the tensile wedging force thus, resulting in earlier crack initiation and a larger final crack. Conversely, compressive residual stress restrains crack formation and thus a smaller final crack.

During the micro indentation, under the contact of diamond shape Vickers indenter, the sample undergoes localized plastic flow that leads to the formation of plastic region. This regime is surrounded by the tensile stress due to the incompressibility of plastically deformed material [62,63]. Since the sign of residual stress formed during CS process is similar to the one created during indentation test, it could enhance the stress and result in larger cracks in the sample with higher residual stress. From the Fig. 19 (a) we can see that the effect of indentation on crack

formation is more in Inconel 625 than in Inconel 718. It is evident from the results we obtained that the surface tensile residual stress has supported the indentation force and resulted in larger cracks whereas for Inconel 718, Fig. 20 (a), it works opposite and resulted in smaller crack. The inset surface profile gives us the depth of cracks measured from the bottom of the indent. Since the measurement was made in the upward direction from the bottom of the indent, lower value of depth with darker color indicated the deeper crack. Cracks are mainly formed around the indents and the depth of cracks are in the size of 8-10 μm. The same samples were investigated after stress relaxation heat treatment and indentation tests were done as shown in Figure 19 (b) & 20 (b). No visible cracks were seen on any of the heat-treated samples. Low porosity and residual stress after heat treatment have contributed on the removal of cracks. As mentioned above, the presence of residual stress could enhance the cracks which is removed after heat treatment. In addition, reduction of hardness and softening of the material could also contribute to the removal of cracks.

In the case of CS deposited Ti-6Al-4V, there is no visible cracks on the as sprayed as well as heat-treated samples as shown in Fig. 21. As mentioned above, the tensile force induced by the indenter could have been restrained by the large compressive residual stress present within the sample.

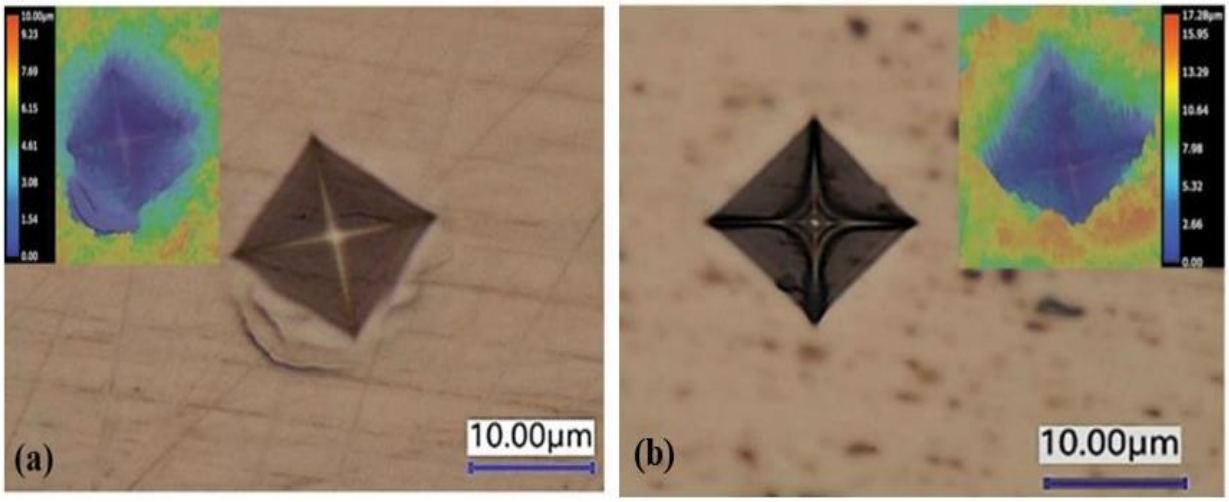

Fig. 19. Vickers indentation on the cross section of CS deposited (a) As sprayed Inconel 625, and (b) Heat treated Inconel 625. Insets shows the surface profile and cracks.

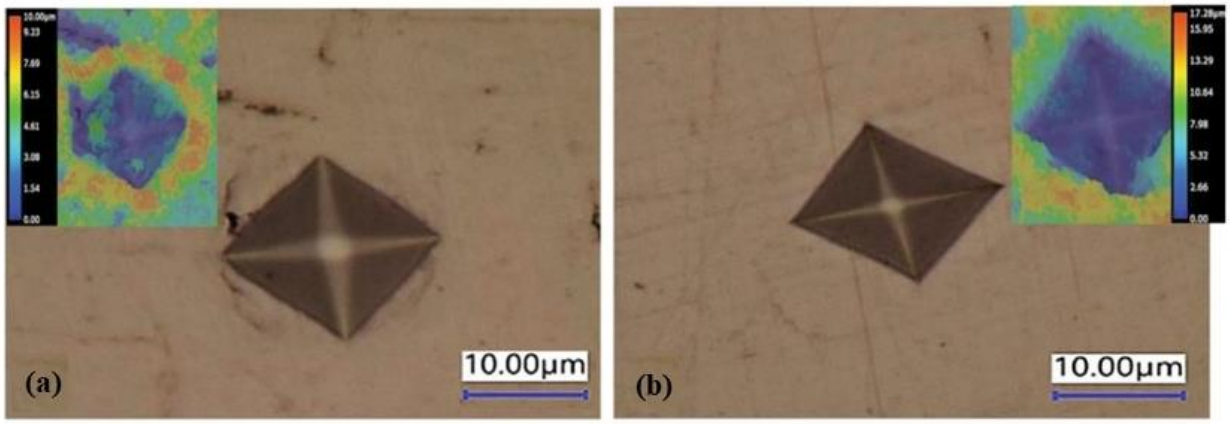

Fig. 20. Vickers indentation on the cross section of CS deposited (a) As sprayed Inconel 718, and (b) Heat treated Inconel 718. Insets shows the surface profile and cracks.

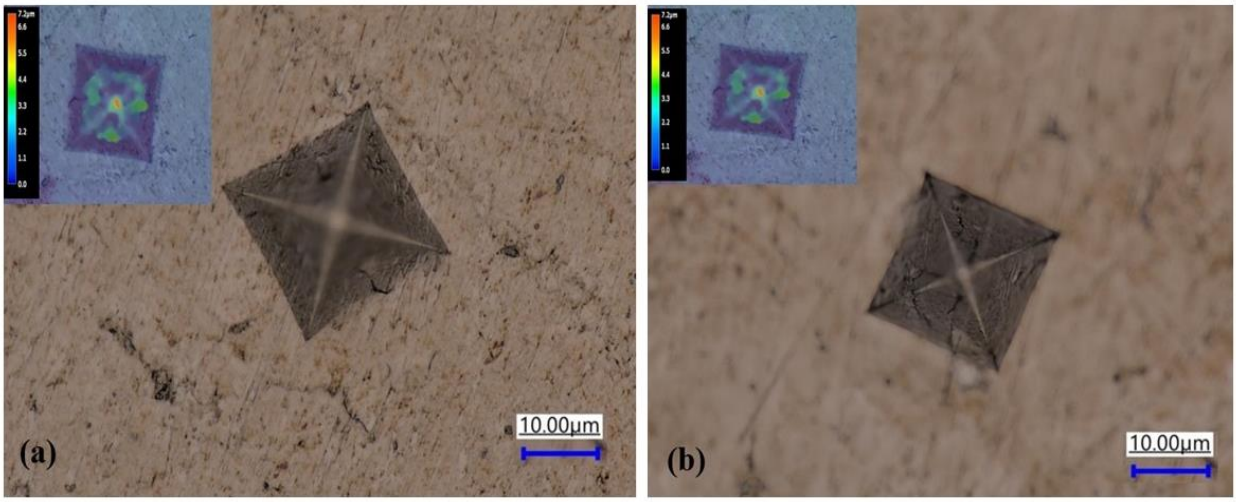

Fig. 21. Vickers indentation on the cross section of CS deposited (a) As sprayed Ti-6Al-4V, and (b) Heat treated Ti-6Al-4V.

5.5. Wear Property

Since no cracks formation was found on the Ti-6Al-4V sample, wear test was performed on the as sprayed and heat-treated sample to examine possibility of establishing wear properties to residual stress formation in the CS deposited titanium alloy samples. The wear rate of the as sprayed Ti-6Al-4V before and after heat treatment were 3.518×10^{-11} m^3/Nm and 4.2157×10^{-11} m^3/Nm, respectively. Wear resistant behavior is dependent on various factors such as composition, hardness, microstructure, porosity content. However, residual stress could be considered as another factor that can affect the wear properties of the materials. Generally, residual stress aid (tensile residual stress) or retard (compressive residual stress) the wear process. Higher wear resistance is accompanied by the increased compressive residual stresses that justifies the result we obtained for Ti-6Al-4V before heat treatment [65]. After heat treatment, the compressive residual stress was relieved, and the hardness was decreased as well. Lower compressive residual stress and lower hardness of the sample could have supported the wear process resulting low wear resistance which agrees with literature [67]. O.P. Oladijo, *et al.* [65] have investigated the

tribological behavior of WC-17Co coatings and found that compressive residual stress retards the wear rate of the material. Hardness is another factor that could affect the wear process of the sample. With the increase in hardness, the wear resistance is increased and vice-versa. Ganesh *et* al. [66], have studied the wear behavior of as-received and surface hardening processes such as shot peening, shot blasting, and age offing ofTi-6Al-4V samples. Hardness after the surface hardening were increased gradually and subsequently the wear resistance of Ti-6Al-4V sample was increased which showed that the hardness has direct relation with the wear behavior. After heat treatment, the hardness is decreased, which resulted in lower wear resistance. This result showed that residual stress could change not only mechanical behavior but also the tribological behavior of materials as well.

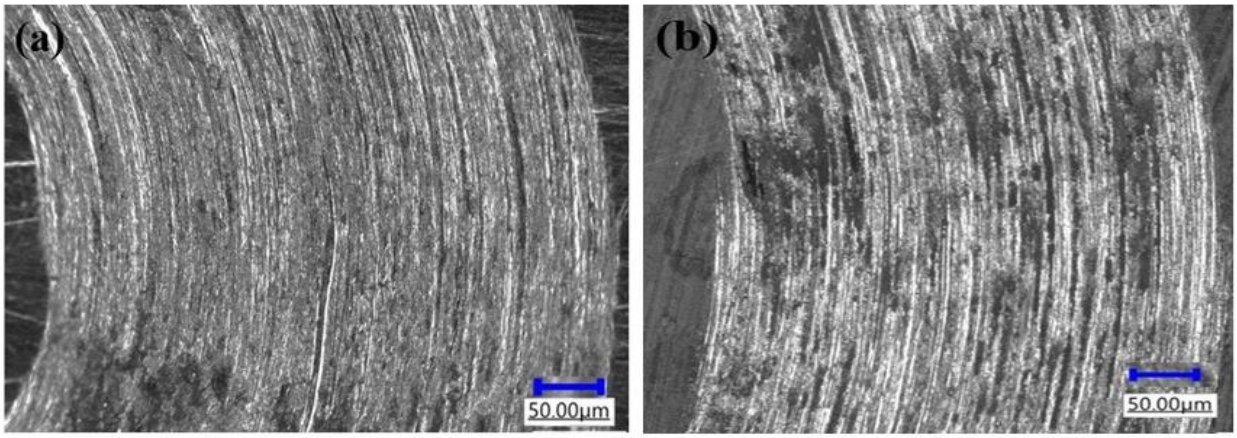

Fig. 22. Micrographs from areas of Ti-6Al-4V sample subjected to wear test (a) as sprayed, and (b) heat-treated.

Fig. 22 (a) and (b) shows the wear morphologies of the Ti-6Al-4V coatings before and after heat treatment on which abrasive grooves are found. Removal of materials from the material surface is attributed to the repetitive sliding of steel balls against the surface [68]. The repetitive sliding of steel balls creates the minute cracks in the subsurface allowing to propagate along the wear track that eventually leads to removal of the material from the deep regions via surface fatigue [69]. The wear track of as sprayed samples exhibits fewer abrasive groves in comparison with the

heat-treated wear track which indicates that the as sprayed samples are more resistant to abrasive and fatigue wear. As sprayed samples are exhibited better resistance to abrasive wear than the heat-treated ones due to the higher hardness and existence of higher compressive residual stress which act against direction of eroding medium during wear test.

6. CONCLUSION

In this study, residual stress formation in three important commercially used alloys (Inconel 625, Inconel 718 and Ti-6Al-4V) during cold spraying process was evaluated. To study the effect of stress relaxation heat treatment on the residual stress, stress relief heat treatment was applied on both Inconel alloys at 800°C and Ti-6Al-4V, 650°C for one hour. Residual stress on Inconel alloys were not uniform throughout the thickness. Measured residual stress by x-ray diffraction method on the surface of CS deposited Inconel 625 was mostly tensile stress whereas, beneath the surface, the residual stress showed a compressive nature. However, in the case of Inconel 718, compressive residual stress was found on both the surface and subsurface regions. However, it is important to mention that residual stress on the surface could be influenced by various factors such as surface treatments therefore, the residual stress on the core of the sample is the main focus of this study. Residual stress on the CS deposited Ti-6Al-4V samples have exhibited compressive residual stress both on the surface and sub-surface similar to the Inconel 718. The porosities were measured for each as sprayed and heat-treated sample. The porosity level was higher in as sprayed Inconel 718 than Inconel 625 which could be the reason for lower hardness. However, titanium being a very porous material itself, showed highest porosity level among the three cold sprayed samples and possess the lowest hardness value. During heat treatment, tensile stresses were induced due to the elimination of porosities within the microstructure of all coating samples. Since the induced stress have opposite sign, it could have canceled out the built-in residual stress that explains the relaxation of the stress after heat treatment. After heat treatment, although porosity level was decreased significantly in all samples, the ha hardness decreased against our expectations. Higher hardness in cold sprayed samples are attributed to strain hardening of metallic particles during the impact and flattening of powders. This process could produce defects such as dislocations within

the microstructure of the coatings after plastic deformation. However, the stress relaxation heat treatment does more than just reduce residual stress by eliminating porosity; it can eliminate dislocations produced by the energy of elevated temperatures. As a result, the hardness of heat-treated samples decreased compared to as sprayed ones. Microstructural observations on both Inconel 625 and Inconel 718 showed some cracks before heat-treatment due to the intentionally made indentations on the cross-sections of the samples. After heat treatment, both Inconel samples did not show any visible cracks which could be attributed to the softening and reduction of residual stress within their microstructures. However, microstructural observation of Ti-6Al-4V did not exhibit any sign of cracks after introducing the intentional indentations on their cross-sections which could be attributed to the presence of highly compressive residual stress. The compressive residual stress works against the tensile stress induced by the indenter during the indentations on the cross-section area. The artificial crack formation was not successful to establish a relationship between residual stress and heat treatment in Ti-6Al-4V samples. To this end, wear test was performed on the CS deposited titanium alloy sample to study possibility of any influence of residual stress content on wear properties of the samples. Wear rate of the as sprayed Ti-6Al-4V was found lower than the heat-treated one. Higher compressive residual stress and higher hardness of as sprayed Ti-6Al-4V could be the reason for lower wear rate compared to the heat treated one that has lower residual stress and hardness.

7. FUTURE STUDY

For the future study, mechanical properties such as strength, fracture toughness, etc. could be studied. We could establish the relation between residual stress and other mechanical properties.

REFERENCES

[1] S. Marx, *et al.*, "Cold Spraying: Innovative Layers for New Applications", *Journal of Thermal Spray Technology*, Vol. 15(2), 2006, p. 177-183.

[2] A. Moridi, *et al.*, "Cold Spray Coating: Review of Material Systems and Future Perspectives", *Surface Engineering*, Vol. 30(6), 2014, p. 369-395.

[3] W. Ma, *et al.*, "Microstructural and Mechanical Properties of High-Performance Inconel 718 Alloy by Cold Spraying", *Journal of Alloys and Compdound*, Vol. 792, 2019, p. 456-467.

[4] O. P. Oladijo *et al.*, "Residual Stress and Wear Resistance of HVOF Inconel 625 Coating on SS304 Steel Substrate", *Journal of Thermal Spray Technology*, Vol. 29, 2020, p. 1382–1395.

[5] A. Al-Hamed *et al.*, "Investigation of HVOF thermal sprayed nanostructured WC-12Co mixed with Inconel-625 coatings for oil/gas applications", *Surface Effects and Contact Mechanics XI*, 215.

[6] F. Chu *et al.*, "Effect of Heat Treatment on Microstructure and Mechanical Properties of Inconel 625 Alloy Fabricated by Pulsed Plasma Arc Deposition", International Federation for Heat Treatment and Surface Engineering 20th Congress Beijing, China, 23-25 October 2012.

[7] D. Srinivasan *et al.*, "Characterization of Cold-Sprayed IN625 and NiCr Coatings", *Journal of Thermal Spray Technology*, Vol. 25(4), 2016, p. 725-744.

[8] C. Lyphout, *et al*., "Residual Stresses Distribution Through Thick HVOF Sprayed Inconel 718 Coatings," *Journal of Thermal Spray Technology*, Vol. 17(5), 2008, p. 915-923.

[9] S.Y. Kim, *et al*., "The Effect of Low Temperature Range Heat Treatment on the Residual Stress of Cold Gas Dynamic Sprayed Inconel 718 Coatings via Neutron Diffraction," *Journal of Thermal Spray Technology*, Vol. 29(6), 2020, p. 1477-1497.

[10] R. Singh, *et al*., "Influence of Coating Thickness on Residual Stress and Adhesion-Strength of Cold-Sprayed Inconel 718 Coatings," *Surface and Costings Technology*, Vol. 350, 2018, p. 65-73.

[11] D. Boruah, *et al*., "Evaluation of residual stresses induced by cold spraying of Ti-6Al-4V on Ti-6Al-4V substrates", *Surface Coatings and Technology*, Vol. 474, 2019, p. 591-602.

[12] P. Cavaliere & A. Silvello, "Mechanical properties of cold sprayed titanium and nickel-based coatings", *Surface Engineering*, Vol. 32(9), 2016, p. 670-676.

[13] D. Boruah *et al.*, "Evaluation of residual stresses induced by cold spraying of Ti-6Al-4V on Ti6Al-4V substrates", *Surface and Costings Technology*, Vol. 374, 2019, p. 591-602.

[14] A. Bowhmik, *et al.*, "On the heat-treatment induced evolution of residual stress and remarkable enhancement of adhesion strength of cold sprayed Ti–6Al–4V coatings", *Results in materials*, Vol. 7, 2020, p. 100119.

[15] C.S. Yip, *et al.*, "Thermal spraying of Ti-6AL-4V/Hydroxyapatite composites coatings: powder processing and post-spray treatment", *Journal of Materials Processing Technology*, Vol. 65, (1997), p. 73-79.

[16] H.R. Salimijazi, *et al.*, "Vacuum plasma spraying: A new concept for manufacturing Ti-6Al-4V structures", *JOM*, Vol.58, p. 50-56.

[17] J. Zhu, *et al.*, "Residual stress in thermal spray coatings measured by curvature based on 3D digital image correlation technique", *Surface & Coatings Technology*, 2011, Vol.206(6), p. 1396-1402.

[18] Y.Y. Santana, *et al.*, "Measurement of residual stress in thermal spray coatings by the incremental hole drilling method", *Surface and Coating Technology*, Vol. 201(5), 2006, p. 2092-2098.

[19] Stress Map. "X-Ray Diffraction (XRD)", www.stressmap.co.uk/x-ray-diffraction-for-measuring-residual-stress/ (Accessed: 7.1.2022)

[20] Gary S. Schajer & Philip S. Whitehead, Hole-Drilling Method for Measuring Residual Stresses.

[21] P.J. Withers & H. K. D. H. Bhadeshia, Residual stress Part 2 – Nature and origins, *Materials Science and Technology*, Vol. 17 (4), p. 366-375.

[22] E.H. Lee, *et al.*, "Residual stresses in glass plate cooled symmetrically from both surfaces", *Journal of the American Ceramic Society*, Vol. 48(9), 1965,p. 480-487.

[23] I.C. Noyan & J.B. Cohen, Residual stress: measurement by diffraction and interpretation. 2013: Springer

[24] G. De Portu, *et al.*, Measurement of residual stress distributions in Al 2 O 3/3Y-TZP multilayered composites by fluorescence and Raman microprobe piezo-spectroscopy", *Acta Materialia*, Vol. 53(5), 2005, p. 1511-1520.

[25] D. Crecraft, "The measurement of applied and residual stresses in metals using ultrasonic waves", *Journal of Sound and Vibration*, Vol. 5(1), 1967. p. 173-192.

[26] M.T. Hutchings, *et al*., "Introduction to the characterization of residual stress by neutron diffraction", *Materials Characterization*, 2007, p. 492.

[27] T. Valente, *et al.*, "Implementation and development of the incremental hole drilling method for the measurement of residual stress in thermal spray coatings", *Journal of Thermal Spray Technology*, Vol.14(4), 2005, p. 462-470.

[28] P. J. Withers & H. K. D. H. Bhadeshia, “Residual stress. Part 1 – Measurement techniques”, *Materials Science and Technology*, Vol. 17(4), 2001, p. 335-365.

[29] I.C. Noyan & J.B. Cohen, Residual Stress Measurement by Diffraction and Interpretation, New York: Springer-Verlag; 1987.

[30] M. Vrana, *et al.*, Neutron Diffraction Measurements of Strain/Stress State Induced by a Weld Deposited Pass http://www.xray.cz/epdic/abstracts/166.html. (Accessed: 7.5.2022)

[31] B. Chen, *et al*., “In situ neutron diffraction measurement of residual stress relaxation in a welded steel pipe during heat treatment”, *Materials science and Engineering: A*, Vol. 590, 2014, p. 374-383.

[32] Shibe & Chawla, Vikas & Research, “An overview of research work in surface coatings”, *International Journal of Research in Mechanical Engineering and Technology*, 2013.

[33] L. Rehorek *et al.*, “Cold gas dynamic spray deposition as additive manufacturing of architecture materials”, *Materials Engineering*, 2018.

[34] X. Wang & K. Chou, “The effects of stress relieving heat treatment on the microstructure and residual stress of Inconel 718 fabricated by laser metal powder bed fusion additive manufacturing process.”, *Journal of Manufacturing Processes*, Vol.48, 2019, p. 154-163.

[35] Z. Chen, *et al.*, “Analysis on Thermal Effect on Residual Stresses of Broached Inconel 718”, *Advanced Materials Research*, Vol. 996, 2014, p. 574-579.

[36] L. Wu & C. Jiang, “Effect of Thermal Relaxation on Residual Stress and Microstructure in the near-surface Layers of Dual Shot Peened Inconel 625”, *Advances in Mechanical Engineering*, Vol. 10(10), 2018, p. 1-6.

[37] C. Lyphout, *et al.*, “Residual Stresses Distribution Through Thick HVOF Sprayed Inconel 718 Coatings”, *Journal of Thermal Spray Technology*, Vol. 17(5), 2008, p. 915-923.

[38] X. Wang & K. Chou, “The Effects of Stress Relieving Heat Treatment on the Microstructure and Residual Stress of Inconel 718 Fabricated by Laser Metal Powder Bed Fusion Additive Manufacturing Process”, *Journal of Manufacturing Processes*, Vol. 48, 2019, p. 154-163.

[39] S.Y. Kim, *et al.*, “The Effect of Low Temperature Range Heat Treatment on the Residual Stress of Cold Gas Dynamic Sprayed Inconel 718 Coatings via Neutron Diffraction”, Journal of Thermal Spray Technology, Vol. 29(6), 2020, p. 1477-1497.

[40] R. Singh, *et al.*, “Influence of Coating Thickness on Residual Stress and Adhesion Strength of Cold-Sprayed Inconel 718 Coatings”, *Surface and Coatings Technology*, Vol. 350, 2018, p. 65-73.

[41] L. Wu & C. Jiang, "Effect of thermal relaxation on residual stress and microstructure in the near-surface layers of dual shot peened Inconel 625", *Advances in Mechanical Engineering*, Vol. 10(10), 2018, p. 1–6.

[42] I. van Zyl, *et al.* "Residual Stress in Ti-6Al-4V objects produced by Direct Metal Laser Sintering", *South African Journal of Industrial Engineering*, Vol 27(4), 2016, p. 134-141.

[43] J. M. Robinson, *et al.*, "X-ray measurement of Residual Stresses in Laser Surface Melted Ti-6A1-4V alloy", *Materials Science and Engineering: A*, Vol. 208, 1996, p. 143 147.

[44] T. Maishurova, *et al.* "Subsurface residual stress analysis in Ti-6Al-4V additive manufactured parts by Synchrotron X-ray diffraction",12th European Conference on Non-Destructive Testing (ECNDT 2018), Gothenburg 2018.

[45] W. Rae & S. Rahimi, "Effect of stress relaxation on the evolution of residual stress during heat treatment of Ti-6Al-4V.", MATEC Web of Conferences 321, 11001 (2020)

[46] V. Papyrin, *et al.*, "Cold Spray Technology" Elsevier, Oxford, 2006

[47] H. Assadi, *et al.*, "Cold Spraying-A materials perspective", *Acta Materilia.*, Vol. 166, 2016, p. 382-407

[48] C.M. Kay & J. Karthikeyan, "High Pressure Cold Spray: Principals and Applications", 2016.

[49] W. Li, *et al.*, "Effect of standoff distance on coating deposition characteristics in cold spraying*", Materials and Design*, Vol. 29 (2), 2008, p. 297- 304.

[50] T. Berruti, *et al.*, "Residual Stresses on Inconel 718 Turbine Shaft Samples after Turning", *Machining Science and Technology*, Vol. 13(4), 2009, p. 543-560.

[51] ASTM E407-07, Standard Practice for Microetching Metals and Alloys. *PA: ASTM International*, West Conshohocken, 2015.

[52] ASTM E2109-00, Test Methods for Determining Area Percentage Porosity in Thermal Sprayed Coatings. *PA: ASTM International*, West Conshohocken, 2017.

[53] ASM Handbook, Vol 4: Heat Treating, ASM International, 1991.

[54] R. Vaben et al., "Correlation of Microstructure and Properties of Cold Gas Sprayed Inconel 718 Coatings", *Journal of Thermal Spray Technology*, Vol. 29, 2020, p.1455-1465.

[55] S. Y. Kim et al., "The Effect of Low Temperature Range Heat Treatment on the Residual Stress of Cold Gas Dynamic Sprayed Inconel 718 Coatings via Neutron Diffraction", *Journal of Thermal Spray Technology*, Vol. 29, 2020, p. 1477-1497.

[56] Standard Test Method for Vickers Hardness and Knoop Hardness of Metallic Materials, ASTM E92 − 17, 2017.

[57] Cold Spray at Plasma Giken Co. Ltd.(www.plasma.co.jp/en/index.html.)

[58] H. Hamatani, *et al.*, "Mechanical and Thermal Properties of HVOF Sprayed Ni Based Alloys with Carbide," *Science and Technology of Advanced Materials*, Vol. 3(4), 2002, p. 319-326.

[59] W. Wong, *et al*., "Cold Spray Forming of Inconel 718," *Journal of Thermal Spray Technology*, Vol. 22(2), 2013, p. 413-421.

[60] F. Azarmi & I. Sevostianov, "Comparative Micromechanical Analysis of Alloy 625 Coatings Deposited by Air Plasma Spraying, Wire Arc Spraying, and Cold Spraying Technologies", *Mechanics of Materials*, Vol. 144, 2020, p. 103345.

[61] L.I. Perez-Andrade, *et al.*, "Optimization of Inconel 718 Thick Deposits by Cold Spray Processing and Annealing", Surface Coatings and Technology, Vol. 378, 2019, p. 124997.

[62] K.L. Johnson, "The Correlation of Indentation Experiments", *Journal of Mechanics and Physics of Solids*, Vol. 18(2),1970, p. 115-126.

[63] X. Chen, *et al.*, "On the Determination of Residual Stress and Mechanical Properties by Indentation", *Materials Science and Engineering: A*, Vol. 416(1), 2006, p 139-149.

[64] Standard Test Method for Wear Testing with a Pin-on-Disk Apparatus, ASTM G99-17, 2017.

[65] O.P. Oladijo, *et al.*, "Correlation between residual stress and abrasive wear of WC-17Co coatings", *International Journal of Refractory Metals and Hard Materials*, Vol. 44, 2014, p. 68-76.

[66] B.K.C. Ganesh, *et al*., "Effect of surface treatment on tribological behavior of Ti-6AL-4V implant alloy", *Journal of Minerals and Minerals Characterization and Engineering*, Vol. 11, 2012, p. 735-743.

[67] W. Luo, *et al*., "Effect of residual stress on the wear resistance of thermal spray coatings", *Journal of Thermal Spray Technology*, Vol. 25(1-2), 2015, p. 321-330.

[68] N.W. Knun, *et al*., "Effect of normal load, sliding speed, and surface roughness on tribological properties of niobium under dry and wet conditions", *Tribology Transactions*, Vol. 57 (5), 2014, p. 944-954.

[69] G.D. Revankar, *et al*., "Wear resistance enhancement of titanium alloy (Ti-6Al-4V) by ball burnishing process", *Journal of Materials Research and Technology*, Vol. 6 (1), 2017, p. 13-32.

[70] V. Luzin, *et al.*, "Through-thickness residual stress measurement in metal and ceramic spray coatings by Neutron diffraction", *Material Science Forum*, Vol. 571-572, 2008, p. 315-320.

[71] D. Boruah, *et al.*, “Evaluation of residual stresses induced by cold spraying of Ti-6Al-4Von Ti-6Al-4V substrate”, *Surface and Coatings Technology*, Vol. 374, 2019, p. 591-602.

APPENDIX. PUBLICATIONS

Peer-reviewed Journal Articles

1. Deepika Shrestha, Fardad Azarmi, and X.W. Tangpong, Effect of Heat Treatment on Residual Stress of Cold Sprayed Nickel-based Superalloys, Journal of Thermal Spray Technology, Manuscript ID# JTST-21-07-4680.R3- ***Accepted*** *(11/11/2021)*

Refereed Conference Papers

1. Deepika Shrestha, Fardad Azarmi, X.W. Tangpong, Effect of Heat Treatment on Residual Stress of Cold Sprayed Nickel-based Superalloys, ITSC 2021— Proceedings of the International Thermal Spray Conference, Montreal, QC, Canada, May 24–27, 2021. (*Invited to submit an extended version to be included in Journal of Thermal Spraying (JTST) after peer review process*)